17 (2025) 100517

Contents lists available at ScienceDirect

Carbon Capture Science & Technology

journal homepage: www.elsevier.com/locate/ccst

Full Length Article

Innovative high temperature heat pump concepts for an economic decarbonization of a carbon capture unit

Shashank Singh Rawat *, Frederico Gomes Fonseca , María Isabel Roldán Serrano

German Aerospace Center (DLR), Institute of Low-Carbon Industrial Processes, Simulation and Virtual Design, Weinbergstraße 10, Cottbus, 03050, Brandenburg, Germany

ARTICLE INFO

Keywords:
Carbon capture
Industrial heat pump
Monoethanolamine (MEA)
Waste heat recovery
Process integration
Electrification

ABSTRACT

Achieving global net-zero emissions requires widespread adoption of Carbon Capture Utilization and Storage (CCUS) technologies. However, the current state-of-the-art using amines relies on fossil fuel-based thermal energy for solvent regeneration, offsetting some emission reductions. This study proposes and validates an economically viable decarbonization strategy for carbon capture units. The carbon capture unit is evaluated in isolation, proposing different cases focused on varying levels of decarbonization. The methodology utilizes available process waste heat while reducing dependence on external heat supply. A techno-economic evaluation against the background of Germany, considering both the high electricity-fuel price ratio and fossil-heavy electrical supply to be important deterrents. Using Aspen Plus™, an industrial pilot CC unit was simulated, and a conventional High Temperature Heat Pump (HTHP) solution employing hydrocarbons was integrated, reducing external heat demand by 27 % with minor process modifications. More complex integration systems can achieve total decarbonization of the heat supply, albeit at higher costs. The study also investigates the role of carbon credits as both a cost and revenue source, along with sensitivity analyses on process costs and emissions. The present work introduces a novel approach for economic decarbonization of solvent-based carbon capture units. Minor modifications to the operating pressure in the regeneration column were found to increase heat demand and emissions, but also permitted the use of novel HTHP technologies, resulting in even lower process costs and emissions at high electrification levels. The results offer valuable insights for researchers, technology providers, and policymakers seeking to reduce emissions from emission-intensive industries.

1. Introduction

In 2021, the atmospheric concentrations of major greenhouse gases reached approximately 415 ppm for CO_2, 1896 ppb (parts per billion) for CH_4, and 335 ppb for N_2O. Notably, the current CO_2 concentrations are known to exceed, with a high degree of certainty, any levels occurring over the past two million years (IPCC, 2023). These unprecedented concentrations, especially of CO_2, are the primary drivers of global climate change. As a result, the frequency and severity of extreme weather events—such as floods, cyclones, wildfires, and storms—have increased in inhabited regions (IPCC, 2023). Beyond these direct impacts on human societies, climate change also leads to significant biodiversity loss and irreversible alterations to natural ecosystems.

To limit global warming potential below 2° C, the energy sector must reduce net CO_2 emissions by 87-97 % by 2050 (IPCC, 2022). The plausibility of retiring fossil-based energy system early seems genuine; however, the local business, individuals and countries might lose economically from their stranded assets. While the feasibility of transitioning to non-fossil energy sources is underpinned by positive intentions, Goh and Gordon (2025) mention the probable push-back from social and industrial players towards policy changes. The Agency (2023) considers retrofitting solutions for currently existent industrial facilities, such as Carbon Capture, Utilization, and Storage (CCUS), crucial short-term solutions particularly for industrial sectors with *unabatable* emissions. These facilities serve as a reliable source of high-purity CO_2, suitable for various applications, including the synthesis of synthetic fuels (Prats-Salvado et al., 2022).

Amine scrubbing is considered as a robust technology for CO_2 removal owing to decades of use and experience in the gas purification industry (Rochelle, 2009). As a benchmark co-sorbent, monoethanolamine (MEA) is characterized by its high cyclic capacity, significant absorption-stripping kinetic rates at low CO_2 concentrations, and high water solubility (Kohl and Nielsen, 1997). MEA reacts readily with aqueous CO_2 to form carbamate, with an absorption capacity

* Corresponding author.
E-mail address: shashank.rawat@dlr.de (S.S. Rawat).

https://doi.org/10.1016/j.ccst.2025.100517
Received 16 July 2025; Received in revised form 5 September 2025; Accepted 6 September 2025
Available online 11 September 2025

Nomenclature

Acronyms

DLR	German Aerospace Center
HP	Heat pump
SI	Supplimentary Information
COP	Coefficient of performance
GCC	Grand Composite Curve
CAPEX	Capital expenditure
OPEX	Operational expenditure
GHG	Greenhouse gas
CCUS	Carbon Capture and Utilization/Storage
HTHP	High temperature HP
MVP	Mechanical vapor recompression
LCOC	Levelized Cost of Carbon Capture
LVC	Lean Vapor Compression
MER-HEN	Maximum Energy Recovery - Heat Exchanger Network
TCM	Technology Center Mongstad
RLHX	Rich-Lean Solvent Heat Exchanger
TAC	Total Annualized Costs (of an industrial unit)
ETS	Emissions Trading System
HX	Heat Exchanger
SRD	Specific Reboiler Duty
AARD	Absolute Average Relative Difference
EUA	European Union Allowances (to be used in the ETS system)
ENRTL-RK	Electrolytic Non-Random Two Liquid model with Redlich-Kwong equation
ELECNRTL	Electrolytic Non-Random Two Liquid model
LMTD	Logarithmic Mean Temperature Difference

Units

ppm	parts per million (mg/kg)
ppb	parts per million (μg/kg)

Latin symbols

E	Cost function exponent
p	price
H	Enthalpy
Q	Heat or enthalpy
$\dot{Q}$	Heat flow rate
t	Tonne (=1000 kg)
T	Temperature
U	Overall heat transfer coefficient
W	Work (energy)
c	Cost
r	Ratio
f	Cost function factor
m	Degression exponent
$\dot{m}$	Mass flow rate
s	Operational cost savings

Greek symbols

Δ	Change or difference between two values of a physical quantity
η	Efficiency
$\alpha, \beta, \gamma, \zeta$	Function coefficients

Subscripts

el	Electricity
fuel	Fuel
lift	Lift
sink	Heat sink side of the heat pump
source	Heat source side of the heat pump
coverage	Heat coverage by heat pump
sys	System integration and peripherals
PI	Planning and installation
om	Operating and maintenance
eq	Referring to a specific equipment
wf	Referring to a working fluid
cap	Referring to captured CO_2
comp,i	Referring to the compressor i
sup	Degree of superheating
sat	Saturated (vapor)
CD	Referring to the condenser in a heat pump
EV	Referring to an evaporator in a heat pump
rec	recovered

of 0.5 mole of CO_2 per mole of MEA (Sema et al., 2012). However, the chemical absorption process generates high reaction heat (approx. 1.9 MJ/kg_{CO_2}), requiring a significant heat supply for solvent regeneration, traditionally carried out using steam stripping (Bravo et al., 2021).

Heat integration analyses in the context of emissions mitigation and carbon capture systems is well-established strategy. Kishimoto et al. (2012) present an alternative pathway in which coal-firing is replaced by coke gasification followed by a CO-shift reaction that yields H_2 for steam-turbine power generation. Using the Linnhoff et al. (1994) pinch-analysis framework, the authors performed a full-scale heat-integration of the combined gasification-CC unit and reported a $\approx$ 40 % reduction in the overall energy demand.

Higgins and Liu (2015) quantify the energetic penalty of several liquid-gas absorption technologies applied to power generation, and showed that modest equipment modifications can increase heat recovery potential. Ali et al. (2018) propose plant wide steam networks that harvest waste heat from hot flue gases and redirect it to the capture subsystem, thereby lowering the net emissions of high intensity industries. These studies focused on improving the exergetic balance of CC units.

High temperature heat pumps focus on the upgrading of waste process heat to useful temperature levels. Currently, there are several options available at different levels of technological maturity. An interesting open-access source of commercial technologies and applications is provided by the IEA HPT (Heat Pumping Technologies, Centre (2023)). Pinch analysis remains the cornerstone for locating the thermal pinch point, marking the boundary between heating and cooling regions, and for the optimal placement of heat pumps. Several works (Townsend and Linnhoff, 1983; Zhang et al., 2015; Linnhoff and Hindmarsh, 1983) highlight the difficulty of integrating vapor compression heat pumps because of temperature lift constraints, a limitation that is increasingly mitigated by modern high temperature heat pump (HTHP) technologies. Alabdulkarem et al. (2015) emphasize the need to co-optimize heat pump selection and working fluid choice.

Recent investigations have therefore explored HTHPs as auxiliaries for amine based post combustion CC. Both upstream and downstream waste heat sources were explored as relevant sources for partial supplementation of the CC heat demand (Hasan et al., 2012; Cremona et al., 2025; Alabdulkarem et al., 2015), as well as CC-specific waste heat, namely the condenser of the regeneration unit (Wilk et al., 2024). Jensen et al. (2024) examined the electrification of an amine based unit for biogas upgrading, combining HTHPs with manipulation of stripper pressure. Isogai and Nakagaki (2024) addressed the high electrical demand of HTHPs by introducing a buffer tank that stores CO_2 rich amine and operates a fully electrified stripper only when grid electricity is economical.

Comprehensive techno economic assessments confirm the viability of these concepts. A cement plant case study by Cremona et al. (2025) compared three HTHP configurations - integrated reverse rankine, lean vapor compression, and mechanical vapor recompression leveraging heat from the cement process, the CC unit, and the intercooler of the downstream CO_2 compressor. Across all scenarios, the inclusion of HTHPs reduced the net heat demand and improved the overall cost effectiveness of the capture system, underscoring the strategic value of advanced heat integration in low carbon energy infrastructures.

However, the possibility of economic decarbonization by detailed analysis of partial to full electrification of a carbon capture unit, using only the waste heat generated within the CC system, has not been explored in the literature so far. Including the decarbonization of large-scale CC projects is paramount to maximize the decarbonization of the entire process chain, which in this case is achieved by electrifying the heat demand of the process. While heat integration offers economic advantages, current proposals rely, at least partially, on upstream or downstream processes or fossil-fuel-based energy, reducing overall efficiency and increasing CO_2 emissions. Thus, an analysis of the CC process as a standalone unit is proposed, which can be either retrofitted into existent industrial units, or considered from the project phase. Further, the CC units are normally supplied as proprietary technologies by the companies. For example, BASF and Linde Engineering worked together to test an advanced solvent OASE Blue for CC with improved process design on a large pilot plant facility (O'Brien et al., 2021). Similarly, Carbon Clean Solutions™ have demonstrated better performance characteristics of their proprietary solvent *CDRmax*™ when compared with MEA (Patkar and Bumb, 2017; Bumb et al., 2017). The aforementioned proprietary technologies are just a few mentioned ones out of the pool of availability to choose from. A comprehensive collection of technologies, not limited to solvent-based CC, is compiled by the Global CCS Institute (Barlow and Shahi, 2024).

Utility requirement is an important decision parameter before proceeding with a unit retrofit, thus it is expected that technology providers disclose this data. This heat demand puts pressure on the existent facilities, and may also lead to lower process outputs (due to rerouting of available process heat) or higher fuel consumption, and thus more emissions. These factors prompt the need for decarbonized variants of currently commercialized carbon capture units.

Both researchers and technology providers alike are called to consider the development of deployable CC units that minimize the need of external heat supply. To maximize the decarbonization potential of the process, care should be given, when possible, to provide electricity with a low-carbon footprint, such as on-site renewable solutions. This paper aims to evaluate an innovative HTHP configuration for ***standalone*** CC units using aqueous MEA solutions, ensuring energy efficiency and minimal additional utility requirements for the existing facility.

1.1. Objectives and novelty

Amine-based carbon capture is a relatively mature technology, but its widespread deployment is hampered by high energy requirements and associated costs. In many retrofit projects the capture unit is supplied with space, power, water and steam from the host plant and is treated as a *black-box* because of proprietary agreements. Consequently, most existing studies evaluate heat-pump integration only when external utilities are available.

The present work investigates the integration of a conceptual reverse-Rankine-cycle-based high-temperature heat pump (HTHP) into a stand-alone carbon capture (CC) plant. Two novel process configurations are benchmarked against the current state-of-the-art using MEA solutions. The specific objectives are:

- **Thermodynamic feasibility:** Establish whether a reverse-Rankine HTHP can be integrated into large-scale CC units without external heat sources based on experimental results from a industrial-scale pilot plant using a CO_2-lean flue gas;
- **Energetic and economic performance:** Quantity the associated cost implications of the HTHP-integrated configurations relative to conventional designs;
- **Design-oriented framing:** Provide a complete analysis of costs and emissions associated with the electrification of carbon capture processes, taking into consideration increased levels of decarbonization as well as minor process operation modifications.

Developing modular CC units for different types of emissions would greatly benefit from not depending on available process heat or utility supply on the overarching industrial unit, permitting higher versatility in applicability, while lowering the efforts for pre-project basic engineering. Prior investigations of heat-pump integration in CC units typically rely on upstream or downstream processes to supply the heat demand. Analyses focused on the electrification of a ***standalone*** CC unit are not absent in the literature, which frequently make use of CO_2-rich flue-gas. Therein lies the novelty of this work, making use of a CO_2-lean flue gas, reflecting the typical emissions of fossil-fuel fired combined heat and power (CHP) units. By highlighting the utility requirements and providing a very conservative estimate for annual costs, the work underscores the techno-economic feasibility of decarbonised variants of commercial CC units and informs technology owners and academic experts alike about realistic integration pathways.

The integration of a reverse-Rankine HTHP into a stand-alone carbon-capture unit promises significant reductions in both energy consumption and operating cost, while preserving the flexibility required for retrofit applications. The subsequent sections of this paper will detail the thermodynamic modelling, the novel plant configurations, and the results of the techno-economic and sensitivity analyses that substantiate these claims.

While the ultimate aim is full electrification of CC units, partial-electrification may be attractive to both prospective clients and technology owners. The concepts presented here can be incorporated into future CC deployments, offering a pathway to reduce the energy penalty that currently limits the attractiveness of amine-based capture technologies.

2. Methodology

This section introduces the fundamentals of the conventional MEA-based carbon capture process, as well as the possible integration of heat pumps. It elaborates on the simulation example central to the paper and elucidates the foundational concept for integrating reverse-Rankine-based HTHP.

As stated in the introduction, one of the main objectives of this manuscript is to provide a novel self-integrated concept for a carbon capture unit. The workflow, presented in Fig. 1, starts with the choice of industrial process targeted for carbon capture, followed by the selection and modelling of the CC process deemed the best for the flue gas characteristics determined in the previous step. The simulation results obtained are validated against reported data from an industrial facility (or literature). The validated simulation model undergoes process integration analysis based on the guidelines proposed by Linnhoff et al. (1994), limiting itself to heat recovery analysis using basic pinch analysis and Maximum Energy Recovery - Heat Exchanger Network (MER-HEN) design. The waste heat analysis (T-Q curves) focuses on individual cooling demand points within the CC unit to identify high-quality waste heat. The results from this method can be translated into the integration of a HTHP system, harnessing available high-quality waste heat to enhance the coefficient of performance (COP). The fundamental process is adapted with diverse heat pump integration concepts. The modified processes are ultimately assessed via a comprehensive technoeconomic analysis and compared with available literature results.

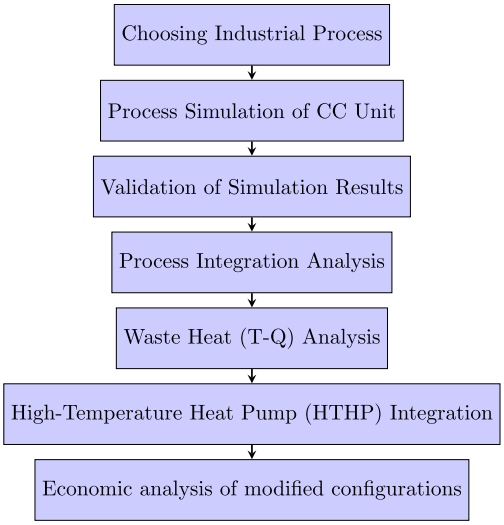

Fig. 1. Workflow for the design of a decarbonization concept applied to a CC unit.

2.1. Carbon capture by chemisorption

The Technology Center Mongstad (TCM) is a test center for developing CO_2 capture technologies and a leading competence center for carbon capture that is located in Mongstad, Norway. It is a joint venture between the Norwegian government and several international oil-and-gas players, with the main goal to evaluate and enhance CO_2 capture technologies in a real industrial setting, ultimately supporting their large-scale implementation. This is done by enabling the technology developers to validate their carbon capture solutions in their facility before full-scale implementation. The facility is designed to process emissions from multiple sources, thus allowing to mimic vast range of different industrial gas composition. Apart from providing testing facility and consultation on carbon capture projects, TCM is active in knowledge sharing through vast number of publication and conferences. The disseminated data provides valuable insight into the operation and process design of a carbon capture unit of high technological readiness (Park, 2025; Mongstad, 2020, 2024).

2.1.1. Process description, plant design and operational parameters

The model discussed in this paper is based on extensive operational data from TCM's 2015 campaign, which treated flue gases from a natural gas-fired power plant and used MEA solvent for carbon capture (CC). This model exemplifies a typical implementation for a chemisorption-based CC plant, following the standard practices outlined by Faramarzi et al. (2017) and can be visualized by Fig. 2. Dimensioning of equipment and stream initialization was carried out based on reported data.

Like all liquid-vapor separation processes, CC features extensive use of contact columns, described in detail in Table S1 in the SI. The direct contact cooler (DCC) is responsible for quenching and lowering the temperature of incoming hot flue gases using water. The quenching also reduces the moisture content of gas and improves the efficiency of the absorption process downstream (Hume et al., 2021).

The absorber employed in the pilot setup features three packing sections and feed positions, which parameters can be customized to maximize testing flexibility (Table S1). In the absorber column, the flue gas comes in contact with the lean solvent and CO_2 is chemically bound to the solvent. The exothermic reaction causes a temperature bulge in the absorber and most of the reaction enthalpy ($Q_{abs,\ CO_2}$) is carried over by the treated flue gas (now CO_2-lean) which is ultimately lost to the environment in the water wash section (Kim et al., 2014).

Two water-wash sections (WW I and WW II, Table S1) are installed above the absorber packing, within the same column. The goal of these units is to quench the sweet gas, lowering its temperature and removing remaining traces of solvent and its degradation products to comply with regulations on gas emissions. The allowable maximum emission limit from TCM plant in perspective of amines was set to 6 ppm_v and that of ammonia to 100 ppm_v (Faramarzi et al., 2017).

The rich solvent (containing chemically bound CO_2) is pumped to the top of the regeneration column (also known as gas stripper), passing through the *Rich-Lean Solvent Heat Exchanger* (RLHX), which performs heat recovery by preheating the pumped rich solvent using the hot lean solvent exiting the regenerator while simultaneously cooling the lean solvent.

The regeneration column is another packed column (Table S1) where the rich solvent is stripped from its absorbed CO_2 using steam. The stripping steam is generated in the reboiler which partially evaporates the amine solution itself (100-140° C), typically using hot utilities at atmospheric or slightly super-atmospheric pressures (low-pressure process steam). The heat demand of the unit ($Q_{reboiler}$) is best described by Eq. (1), where $Q_{sensible}$ refers to the heat required to raise the temperature of the incoming rich solution between RLHX output and reboiler temperatures; and $Q_{vap,\ H_2O}$ refers to the heat of evaporation necessary to generate the portion of stripping steam in the reboiler that does not condense as it rises through the stripper column and eventually condenses in the overhead condenser (Oexmann and Kather, 2010).

$$Q_{reboiler} = Q_{sensible} + Q_{vap,\ H_2O} + Q_{abs,\ CO_2} \quad (1)$$

The stripper considered in this model operates at a pressure of around 1.9 bar_a and the reboiler supplies the required energy using condensing 3 bar_a steam. The hot lean solvent is pumped again through the RLHX, usually still requiring the supplementation of cold utilities to reach the desired absorber temperatures. The stripped gas (having large proportion of CO_2) leaves the top of the stripper packing and enters the water wash section (WW III, Table S1), which operates similarly to WW I and WW II, removing solvent and amine degradation products (Morken et al., 2017), as well as contributing visibly to the recovery of CO_2. Unlike the water wash sections after the absorber where the emissions are to be tuned to the environmental standard, the water wash section after the stripper contributes to an extent to maintain the CO_2 product quality. The washed gases after the stripper are partially condensed using cold utilities to remove water and amine, which are refluxed to the column (Johnsen et al., 2019). The overhead production is the target conditioned CO_2 gas.

With a carbon capture unit being an end-of-pipe solution, the existing utility system is often unable to fulfill the additional energy demand of the retrofit. Process steam using in the TCM pilot is sourced from an upstream refinery. The estimation of cooling water temperature was done based on the report prepared by Golmen et al. (2013), which carried out various sea parameter measurement for two years (2011-2013). Based on the annual undersea temperature (at a depth of 100 m) off the coast of Mongstad, it was assumed in this study that the cooling water intake is at 10° C and discharge is at 15° C.

The process description tells us that while there is a single spot requiring heat demand (reboiler), there are several points throughout the system where cooling is needed (lean amine cooler, WW I, II, and III, DCC cycle cooler, and regeneration condenser). These are clear potential points for heat integration, with the main issue being the stark mismatching between temperature levels for these streams.

2.2. Aspen Plus™ modelling of the TCM unit

This section discusses the steady-state simulation in Aspen Plus™V14 for the CC unit described in Section 2.1.1. The thermodynamic property method used in the entirety of this analysis is the electrolytic non-random two liquid with Redlick-Kwong gas (ENRTL-RK) method, a common solution found in the literature (Smahi et al., 2023; Sanku and Svensson, 2019). The section on simulation validation Section 4.1 covers different model comparison in detail later. Acid-base chemistry

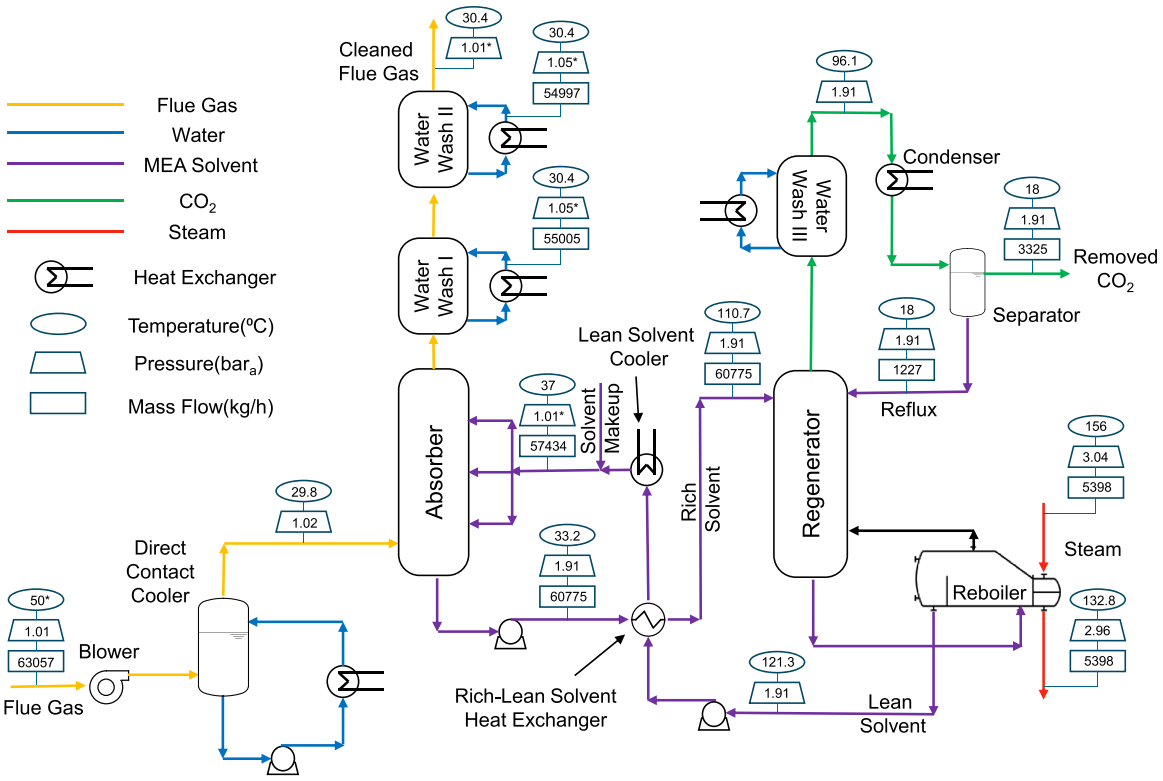

Fig. 2. *State of the art: MEA based carbon capture system*- The indicated process parameters are based on MEA testing results from the technology centre Mongstad's CHP-flue gas CO_2 capture test campaign Faramarzi et al. (2017). The specified values in figure as * are assumed for simulation purposes.

Table 1
Flue gas characteristics defined in the simulation (Adapted from Faramarzi et al. (2017)).

Flow rate	m^3/h	59,430
Temperature	˚C	50
N_2	Std.Vol%	77.86
O_2	Std.Vol%	14.6
CO_2	Std.Vol%	3.84
H_2O	Std.Vol%	3.70

and reactions were taken from the example simulation provided by Aspen Technology (2014). Detailed descriptions of unit blocks, species, utilities, and reactions are available in chapter S2 of the Supplementary Information (SI), while important process parameters for simulation initialization can be found in chapter S1.

2.2.1. Process flow and unit operations

Feed Stream (Flue gas): The flue gas is taken from the stack of the power plant, with the characteristics presented in Table 1. While the literature mentions exhaust flue gas temperatures for large-scale CHP systems between 149 and 185˚C (Hume et al., 2021; U. S. Environmental Protection Agency and Heat, 2015), it was decided to assume a lower temperature to allow the simulation findings to be applicable to wider varieties of flue gases. The methodology described earlier (Fig. 1) could flag such upstream high-temperature flue gases as high-quality waste heat. To avoid assumptions about industrial heat recovery, lower flue gas temperatures are used, keeping the analysis at the carbon capture unit level and providing a conservative scenario.

Direct Contact Cooler: It is assumed that the flue gas is taken from the bottom of the stack at atmospheric pressure, and is pressurized by a blower to overcome pressure losses in the upcoming columns. Actual pressure losses calculations were not considered for this stage, and a value of 1 kPa was assumed. The direct contact column (DCC) is modeled as an Equilibrium-based *RadFrac* unit block, where flue gases enter from the bottom stage and quenching water enters from the top stage. The mass flow is estimated using a *design specification* to ensure a final temperature of 29.8˚C. Relevant parameters for the water washing cycles can be found on Table S3 in the SI.

Absorber: The Absorber column is modelled as a Rate-based *RadFrac* unit block, maintained at atmospheric pressure without any assumed pressure drop. In the context of this manuscript, a single feed at the highest feed position was assumed, and the packing was assumed to be a single unit 24 m tall (Table S1). The unit block also contains the water washing stages (WW I + WW II) associated with the absorber, where reaction is not assumed to take place; relevant parameters for the water washing cycles can be found on Table S3 in the SI. The corresponding hydraulic plots produced by the software indicated correct dimensioning, by presenting an estimated flooding of less than 80 % throughout the entire column. CO_2 lean flue gas exits the top of the absorber column at atmospheric pressure and rich amine solvent (CO_2-loaded) exits via the bottom stage.

The CO_2 capture rate can be estimated using Eq. (2), where $\dot{F}_{CO_{2,i}}$ refers to the molar flow of CO_2 in a given gas stream *i*. It is also one of the methods summarized in Table S14 of SI.

$$\eta_{CO_2} = \frac{(\dot{F}_{CO_2,flue} - \dot{F}_{CO_2,sweetgas})}{\dot{F}_{CO_2,flue}} \quad (2)$$

Regeneration: This column is also modelled as a rate-based *RadFrac* unit block, maintained at 1.91 bar_a without any assumed pressure drop. Plant data from the 2015 TCM Campaign using MEA and power plant flue gases were used to parameterize the simulation (Faramarzi et al., 2017; Montañés et al., 2017). A reboiler duty ($\dot{Q}_{reb}$) of 3417 kW from Montañés et al. (2017) was adopted, as it slightly exceeds the 3323–3390 kW range in Faramarzi et al. (2017), providing a conservative allowance for operational variability and design.

The hot rich amine solvent, from the RLHX (see Section 2.1.1), is fed to the top of the reactor area together with the reflux from the overhead condenser. The reboiler is modelled as a kettle to facilitate convergence, although Montañés et al. (2017) mentions that the reboiler employed in the real plant is actually a thermosiphon. The diameter of the columns in this stage is defined as 0.92 m, although the actual reported value is 1.25 m (Table S1), to achieve satisfactory results for the hydraulic plots by limiting flooding in each stage to less than 80 %, i.e., within normal allowed operational limits. The regenerated lean-amine solution exits through the bottom stage (reboiler) of the regeneration column and is *heat integrated*with the RLHX, as described in Section 2.1.1.

The acid gas water washing on top of the regenerator (WW III) is contrarily to what is observed for the absorber column, modelled as a separate unit block with no pressure losses, in opposition to the strategy adopted when modeling the absorber. It operates similarly to the aforementioned water washing cycles, relevant parameters for the water washing cycles can be found on Table S3 in SI.

The specific reboiler duty(SRD) is an important performance parameter of a CC unit. It can be typically estimated using Eq. (3), where $\dot{m}_{CO_2,rec}$ refers to the mass flow of CO_2 leaving the condenser of the regeneration column.

$$SRD = \frac{\dot{Q}_{reb}}{\dot{m}_{CO_2,rec}} \tag{3}$$

CO_2 conditioning: The gases exiting the WW III are primarily comprising of water and CO_2. These are cooled down using an overhead partial condenser employing cooling water, with the temperature defined to ensure a moisture value within target values in the final CO_2 product. Separation occurs in an adiabatic flash tank and the bottom reflux is recycled to the regenerator column.

MEA Make-up: After integration in the RLHX, the lean amine requires further cooling to achieve the temperature requirements for the absorber (35° C). The makeup unit block estimates automatically the necessary amount of MEA and water that needs to be supplied to the system to maintain standard 30 wt.% of MEA while compensating for losses due to evaporation. Losses due to chemical degradation have not been considered within the context of the model.

2.3. Economic analysis

2.3.1. Capital cost

The base equipment cost is calculated considering the component size, construction material, design pressure and temperature, base purchase cost and its reference year. Base costs (C_b) are obtained from available literature (Smith, 2005; Peters et al., 2003) and equipment costs (C_d) have been calculated according to Eq. (4), where the reference capacity (CAP_b), capacity factor of each component (F) and additional correction factors (Table S17 in the SI) related to the construction material (f_M), design temperature (f_T) and pressure (f_P) are included (Smith, 2005). These factors are listed in Table S17 in SI.

$$C_d = C_b \left(\frac{CAP_d}{CAP_b} \right)^F f_M f_T f_P \tag{4}$$

The installed equipment costs ($CAPEX_{eq}$) are obtained by applying installation factors to the base equipment cost (Table S17 in the SI), as well as bringing the costs up to the cost year using Chemical Engineering Plant Cost Indexes (CEPCI, Maxwell (2025)). Thus, the CAPEX of an equipment can be estimated using Eq. (5), where f_{ins} is the installation factor, estimated using Eq. (6) (Ali et al., 2018).

$$CAPEX_{eq,2024} = C_d \times \left(\frac{CEPCI_{2024}}{CEPCI_{ref}} \right) \times f_{ins} \tag{5}$$

$$f_{ins} = f_{ER} + f_{IC} + f_{EL} + f_U + f_{OS} + f_B + f_{SP} + f_{DEC} + f_{CONT} + f_{WS} \tag{6}$$

2.3.2. Yearly operation and maintenance costs

Operation and maintenance (O&M) costs or operation expenses (OPEX) consider both fixed and variable costs (Eq. (7)), and are typically reported in reference to 1 operating year. Fixed costs do not vary in the short term and do not depend on the units of materials consumed or produced, and include maintenance and labor costs. Maintenance costs are defined as 4 % CAPEX and labor costs are calculated according to the average yearly salary of one engineer and 3 operators.

$$OPEX = \sum Fixed_{OPEX} + \sum Variable_{OPEX} \tag{7}$$

Variable operating costs include the input materials required to operate the unit, such as utilities and fresh feedstock (Aromada et al., 2020). In the process in question, the considered utilities are electricity (fan, pumps, and compressors), low-pressure steam (reboiler) and cooling water (cooling system), while fresh feedstock includes make-up water, MEA and working fluid.

MEA make-up is assumed to be 1.5 $kg/t_{CO_{2,cap}}$ (Morken et al., 2017). To maintain an MEA concentration of 30 wt.% MEA solution at the lean input, the make-up unit block (Section 2.2) reports the water and MEA requirements over time.

In addition to that, a value of 1 % blow-down of the total volume flow is assumed for processes using direct quenching (DCC, WWs) (Asian Development Bank, 2022). The cooling water makeup is assumed at 2.9 % of total cooling water requirement owing to evaporation, windage, and blow-down losses (Asian Development Bank, 2022).

The assumed cost parameters can be seen in Table S18 in SI. Thus, variable operating costs are estimated considering the yearly item consumption, specific unit price and plant operating hours per year. Steam costs have been calculated considering the price of the natural gas and evaluating the natural gas consumption required for the annual steam production assuming an efficiency of 82 % (Husebye et al., 2012). Following Ali et al. (2018), the costs for CO_2 transport and storage are not included in the OPEX evaluation.

To estimate the total annual cost, it is important to estimate the annualized CAPEX of the plant. This can be achieved using Eq. (8), where n represents the operational year and r is the interest rate, assuming a construction time of 1 year and 24 years of operation (Table S18 in the SI, Ali et al. (2018)).

$$Annualized\ CAPEX = \left[\frac{\sum CAPEX_{eq}}{\sum_{n=1}^{24} \left(\frac{1}{(1+r)^n} \right)} \right] \tag{8}$$

The total annualized cost of the plant (TAC) is, therefore, given by Eq. (9) (Ali et al., 2018):

$$TAC = OPEX + Annualized\ CAPEX \tag{9}$$

2.3.3. CO_2 capture cost

The levelized cost of carbon capture (*LCOC*) is a common metric for evaluation of CC processes, referring to the cost of removing a certain amount of CO_2 from a gas stream, traditionally reported in $Tonne_{CO_2}$. It can be estimated using Eq. (10)), where $\dot{m}_{CO_2,cap}$ refers to the mass flow of captured CO_2, i.e., the difference between the value present in the feed gas and that present in the exhaust sweet gas (Aromada et al., 2020).

$$LCOC = \frac{TAC}{\dot{m}_{CO_2,cap}} \tag{10}$$

CHP power plants within the European Union are required to take part in the European Union Allowance (EUA) system (European Commission, 2014). Within this system, emitting industries are allocated a specific amount of EUA, where each EUA stands for the emission of 1 $Tonne_{CO_2}$ (1000 kg). Fees and other penalties may be incurred if a unit does not have enough EUA to account for their emissions. On the other hand, EUA can be traded through the European Emissions Trading System (ETS), allowing for possible new sources of revenue for

environmentally-friendly projects, while permiting more polluting industries pay for the right to emit. It must be kept in mind, that a finite amount of EUA is made available by the European Union per year, and this amount decreases every year (Federal Ministry for Economic, 2023). The value of each EUA is assumed to be 63.32 €/t_{CO_2} (value referring to mid December 2024, International Carbon Action Partnership (2025)). In the context of this TEA, an initial pool of around 31,000 EUA (around 1.96 M€/y), corresponding to the input flue gas is available. All Scope I emissions (associated with fuel use and non-captured emissions) count as further *ETS costs* for the purposes of this work, while Scope II emissions, such as those associated with the electrical grid, are not considered for this estimation. It is assumed that remaining EUA after accounting for *ETS costs* can be issued as certificates and traded away within the ETS system, thus being considered as *ETS revenues*.

3. Valorization of high-quality process waste heat

The Aspen Engineering Package™ includes the Aspen Energy Analyzer™, an add-on which facilitate pinch analysis of the results of a simulation carried out in Aspen Plus™, determining the pinch point and tracing process composite curves and the Grand Composite Curve (GCC), which can be interpreted as the heat flow requirement at a given temperature after implementing heat recovery principles (Walden et al. (2023)). The software is also able to estimate and visualize different feasible HEN designs, based on different optimization criteria, such as number of heat exchanger (HX) units, CAPEX, and practicality of implementation. In the case of the process in study, temperature level leaps between the heating and cooling regions make any MER-HEN design other the one already present impractical.

3.1. Strategy for high-quality waste heat utilization

The following step in the decarbonization workflow (Fig. 1) focuses on the analysis of individual points of available process heat, that is currently removed using cooling utilities. This analysis is done with the help of the T-Q curves obtained for each HX, allowing for the identification of interesting heat sources to be upgraded using heat pumps. Two relevant cases can be readily identified: the overhead condenser of the regeneration column, due to the high temperature level and substantial latent heat potential; and the DCC cooler, due to the high sensible heat potential. The values of the cooling requirements and heat potential for each HX can be found in the SI (Table S8). An example of the waste heat utilization strategy can be found in Fig. 3(a), where the T-Q for the overhead condenser is presented. The area between the process T-Q curve (red) and the cold utility translates to the concept of irreversibility with the heat exchanger, where higher irreversibility translates to higher exergy destruction (Bejan, 1982; Itoh et al., 1986).

A Python tool was developed *in-house* to identify constant temperature levels at which heat extraction can be maximized while minimizing the irreversibility area. Constant temperature levels correspond to phase changes, such as the two-phase region of a working fluid, like the evaporator of a reverse-Rankine-cycle based heat pump. Temperature level selection is made assuming a ΔT_{min} of 5° C, and targets a heat recovery of 2/3 of the available heat, as shown in Fig. 3(b). The remaining low-grade waste heat can, then, be taken away by the cold utility. As depicted by the shaded areas, the irreversibilities associated with the approach in Fig. 3(b) are much lower than the base case shown in Fig. 3(a).

There are situations where the available waste heat within a single source does not cover the demand of the target heat sink. In such cases, a multi-stage heat pump solution can be considered, as exemplified in Fig. 3(c). The selection of the second temperature level is not governed by the same logic as of the first temperature level, as the only criterion to define the energy availability at the second level is to maintain a minimum temperature difference of ΔT_{min} of 5° C at one end of the heat exchanger. The remaining waste heat is again removed by the available cold utility. Although Fig. 3 only depicts the overhead stripper condenser, it is implied that the heat uptake at higher temperature levels can be extended to other heat sources available in the system.

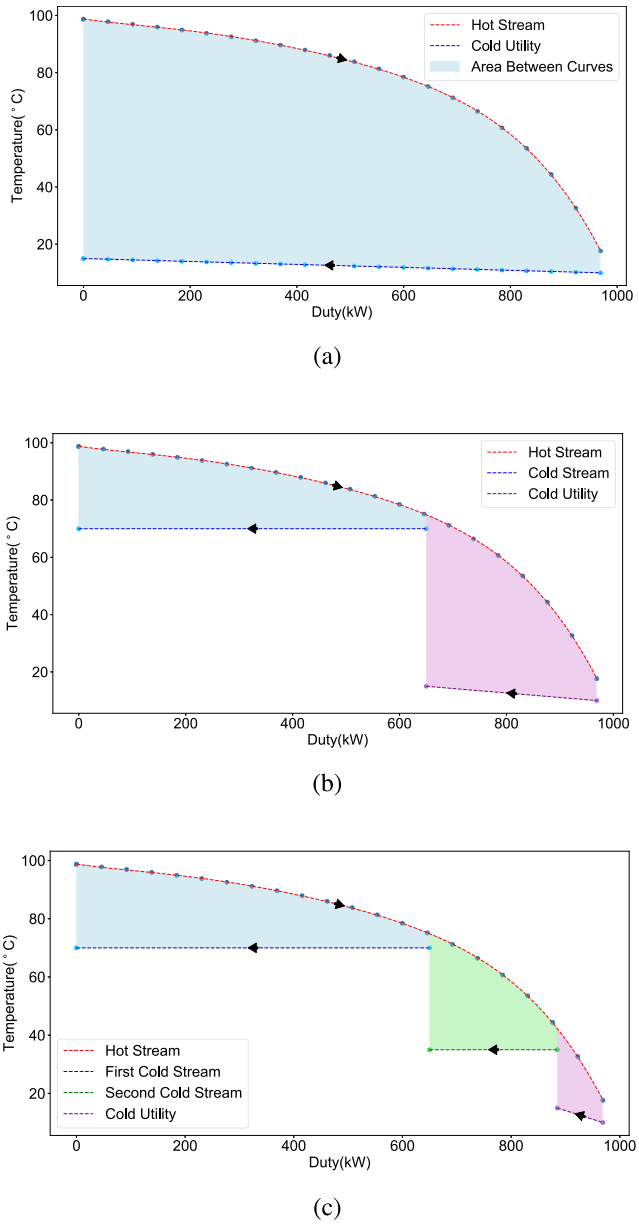

Fig. 3. T-Q curves of the overhead condenser of the regeneration column. (a) No heat pump implementation; (b) Proposed constant temperature heat uptake for a single-stage concept; (c) Proposed constant temperature heat uptake for a two-stage concept.

It is important to notice that, although decreasing irreversibilities within the heat exchanger helps utilization of higher quality of waste heat, it also leads to increased cost, due to a lower LMTD, leading to larger transfer areas. Moreover, additional equipment leads to higher costs, as the heat load of a single HX is now covered using multiple larger HXs.

3.2. High-temperature heat pump integration

The target of the heat pump is to lower the current steam demand in the regeneration column reboiler, based on heat integration strategies considered state-of-the-art in gas-liquid separation (Díez et al., 2009).

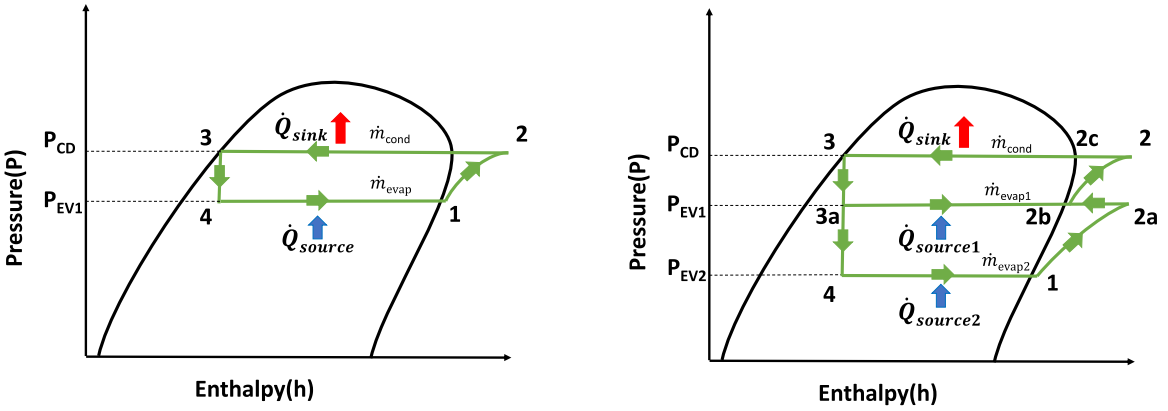

(a) Single-stage HTHP with single heat source

(b) Two-stage HTHP with intermediary heat source

Fig. 4. Log P-h curves for the working fluid within HTHP concepts.

The same tool described in Section 3.1 is able to estimate heat pump parameters after minimizing the irreversibilities and determining the characteristics of the heat source(s) and sink. The tool makes use of the *CoolProp* (Bell et al., 2014) module, and makes use of all 123 working fluids available in the *CoolProp* library. The implementation is able to filter working fluids and is able to determine state variables at different points of the heat pump, for detailed modelling or troubleshooting, as well as key process parameters. Two relevant filtering criteria are considered: 1. only pure working fluids were considered for this analysis; 2. the heat sink temperature is at least 15 K below the critical temperature of the working fluid. Other relevant assumptions made during the programming of the tool are as follows:

(a) Reverse-Rankine cycle based heat pump;
(b) Isentropic efficiency of compressor is set at 72 %;
(c) Isenthalpic expansion is assumed for the working fluid via throttling valves;
(d) After compression, $\Delta T_{sup} \geq 5$ °C;
(e) No supercooling on the condenser;
(f) Assumes ideal state of mixing for working fluid, i.e.; ΔH_{mix} (Enthalpy of mixing) = 0.

This tool is currently under development and is the subject of a future manuscript being composed at the time of writing.

Two reverse-Rankine cycle design concepts were considered, a single-stage (Fig. 4(a)) and a two-stage (Fig. 4(b)) heat pump system. In the case of the single-stage HTHP, the total mass flow of working fluid ($\dot{m}_{wf}$) is given by the available source heat.

In the case of the two-stage HTHP concept, the total mass flow of working fluid ($\dot{m}_{cond}$) is decided by the fraction of the heat demand intended to be covered by the heat pump ($\dot{Q}_{sink}$), supplied by the isobaric enthalpy change *2-2c-3* (see Fig. 4(b)). The temperature levels estimated in Section 3.1 (Fig. 3(c)) determine the operating pressure for the two evaporators (P_{EV1} and P_{EV2}). Mixing of $\dot{m}_{evap1}$ (middle pressure level) and $\dot{m}_{evap2}$ (lower pressure level) is estimated so that point *2b* presents a degree of superheating of 5° C above saturation, leading to a value of $\dot{Q}_{source1}$ lower than the equivalent in a single-stage heat pump (H_{2b} - H_{3a}). The mass split at point *3a* is estimated based on the enthalpy ratios between the two levels (see Fig. 3(c)).

It is difficult to estimate the material loading of a heat pump *a priori*. Data gathered by the IEA Heat Pumping Technologies (Centre, 2023), estimates fluid charges of 8 kg/kW for hydrocarbons and 2.86 kg/kW for ammonia. Yearly losses of working fluid were estimated as 3.77 vol.% of the fluid charge (Eunomia Research Consulting Ltd, 2014). These values are considered derisory in comparison to the total yearly costs of the unit, and were not factored into cost analysis.

3.3. New process configurations

This section aims to visualize changes in process configuration with the integration of HTHP into the existing CC unit. The three electrification variants of the simulated TCM CC unit (V1.0) are named as V1.1 (single-stage pump), V1.2 (two-stage, 50 % electrification), and V1.3 (two-stage, 100 % electrification). A new case (V2.0) is characterised by a regenerator pressure of 1 atm, for which no experimental data is available for validation, with the variants named V2.1, V2.2, and V2.3. Jensen et al. (2024) mentions that lowering the stripper pressure is known to increase the specific reboiler duty (SRD), while also making a strong case for integration of heat pumps, and Mullen et al. (2024) remind us that lowering the reboiler pressure would lead to higher material losses of amine and water. Although seemingly counterproductive, lowering the stripper pressure in a carbon capture unit also lowers the temperature lift (ΔT_{lift}) provided by a heat pump making use of condenser waste heat as its main heat source, despite leading to a higher SRD. This reduced ΔT_{lift} subsequently decreases the pressure lift required, resulting in lower compressor work (W_{comp}) and a higher coefficient of performance (COP, Eq. (11)), thereby facilitating the integration of efficient heat pumps. This, in turn, enhances the electrification potential of the carbon capture unit and enables a potential shift towards a decarbonized heat supply, despite the associated increase in energy demand.

$$COP = \dot{Q}_{sink}/W_{comp} \tag{11}$$

Situations for which the total heat demand of the reboiler cannot be supplied using the HTHP hinge on the fact that the original reboiler can be split into separate parallel HX, where one is supported by the heat pump, and the other by process steam. Luyben (2018, 2022) discusses feasibility of installation and operation of split parallel reboilers like the ones considered in this work. For such applications, thermosiphon reboilers are recommended due to lower fluid inventories. The possibility of installing two heat sources in a single thermosiphon is discussed by Martin and Sloley (1995). In any case, the reboilers considered in this work were modeled as parallel kettles to facilitate TEA.

As expected, single-stage variants (V1.1, V2.1) employ 2/3rd of the highest quality waste heat available, in the overhead condenser, to partially cover the reboiler heat demand, leading to a splitting of this condenser into two HX. This corresponds to the irreversibility case presented in Fig. 3(b), and the thermodynamic cycle presented in Fig. 4(a).

The second electrification concept (V1.2, V2.2) is portrayed in Fig. 5(c) and (d) which aims to provide 50 % of the reboiler duty. As the first electrification concept is unable to cover this heat demand using a single heat source, extra heat at a lower temperature level was utilized

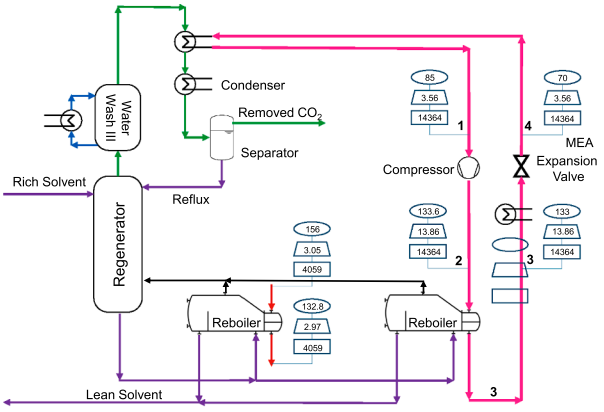

(a) Single-stage variant with isopentane as a working fluid (V1.1)

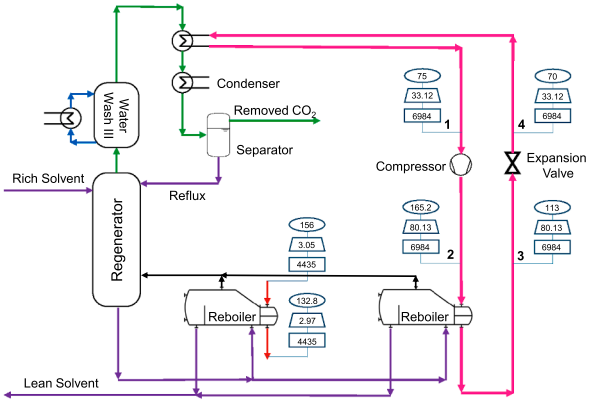

(b) Single-stage variant with ammonia as a working fluid (V2.1)

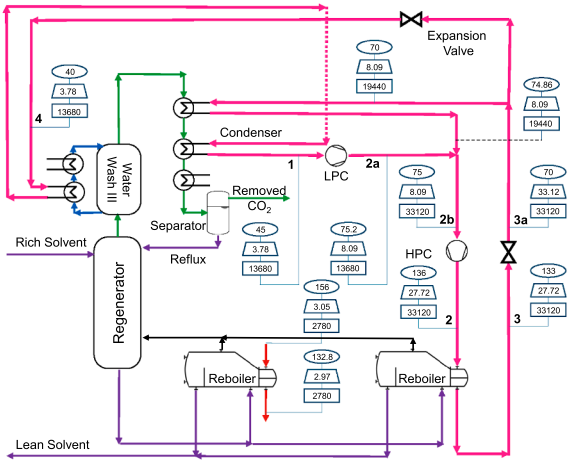

(c) 50% Electrified variant with *n*-Butane as a working fluid (V1.2)

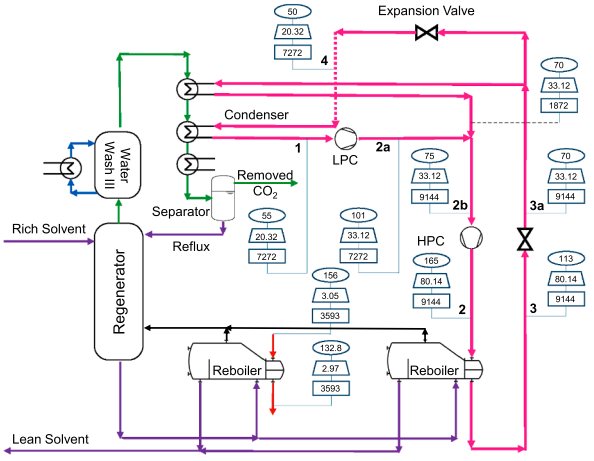

(d) 50% Electrified variant with ammonia as a working fluid (V2.2)

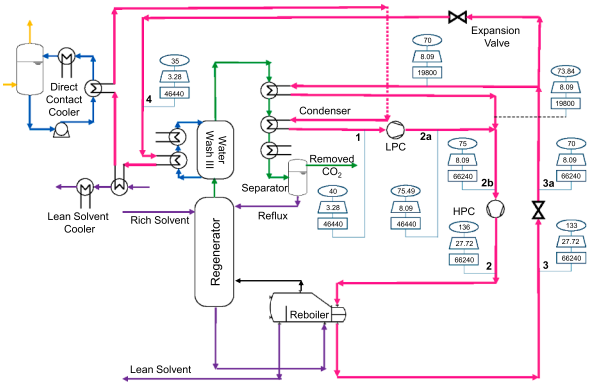

(e) 100% Electrified variant with *n*-Butane as a working fluid (V1.3)

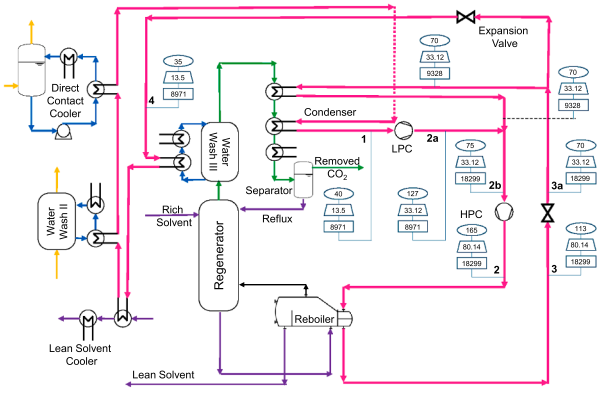

(f) 100% Electrified variant with ammonia as a working fluid (V2.3)

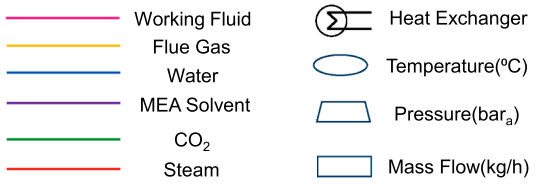

Fig. 5. Process configuration proposals for HTHP integration within the CC unit.

by splitting the overhead condenser into three HX, following the concept presented in Fig. 4(b). One portion of the cooling duty is provided by the evaporating working fluid of HTHP at high temperature, second portion again by split working fluid of HTHP at low temperature and remaining by cold utility as shown in Fig. 3(c). The process employs two partial merged heating fluid loops at different pressure levels, requiring thus either two compressors or a multi-stage compressor with intermediate intake, which is not unheard of in heat pump contexts (Xu et al., 2022).

The third electrification concept (Fig. 5(e) and (f)) aims at the complete internal integration of the CC unit. The concept is similar in execution to the second electrification concept, but larger amounts of heat are upgraded by allowing the lower stage of the thermodynamic cycle (Fig. 4(b)) to remove low quality sensible heat from several points in the system. Apart from the low temperature heat sources in the previous case, waste heat from the lean solvent cooler and direct contact cooler is also utilized for variant Fig. 5(e). The variant Fig. 5(f) in addition to aforementioned low temperature heat sources, also draws on waste heat from Water Wash II of absorber. The criterion for waste heat uptake at lower temperature is directly related to fulfilling the total energy demand on the sink side. This requires dividing each affected HX into two or more units, increasing capital costs. Contrarily to the other concepts, the third concept assumes the use of a single reboiler for the regeneration column.

Several of the process streams present in the system imply the use of corrosion-resistant materials, namely due to the reactivity of amine solutions. The overall heat transfer coefficient (U-value) is estimated based on the phenomena happening within, namely the nature of the fluids, the type of HX and whether phase change occurs. These values can be found in Table S2 in the SI. Based on this data, it is possible to estimate the area of each new HX for each configuration.

4. Results

4.1. Validation of the base process model

A steady-state digital twin of the TCM CC pilot plant facility was created using Aspen Plus™, as described in Section 2.2. The model outputs can be used to validate the simulation. Four simulation models were considered for this based on the different thermodynamic models or altered physical properties database.

- Model I- The Aspen Plus V14 ENRTL-RK model was taken as it is based on the example file of industrial scale carbon capture unit (Aspen Technology, 2022);
- Model II- Aspen Plus V14 ELECNRTL thermodynamic model was chosen as the default available method in the properties environment (Aspen Technology, 2014);
- Model III- The updated e-NRTL model was employed, incorporating revisions to the physical properties database within the default ELECNRTL framework, as recommended by Nakagaki et al. (2019). This framework was also used by Cremona et al. (2025) in their simulation work;
- Model IV- The fourth kind of model has been rigorously developed to correctly represent physical properties of MEA CC systems by Morgan et al. (2018, 2012–2022). The physical property framework is imported from the aforementioned Aspen file, and the TCM unit's simulation model is run in this updated physical property environment.

A comprehensive evaluation of the four simulation models is presented in Table S15 in the SI. Relevant deviations are observed in key parameters, namely the sweet gas temperature, lean CO_2 loading, regenerator column reflux rate, product CO_2 flow rate, and subsequently, SRD. The analysis reveals that Model II exhibits the lowest average deviations, indicating that it is the most accurate representation of the TCM's steady-state behavior, followed by Model I. Despite these results, Although Model II showed more favorable validation, Model I was selected for this analysis due to its accuracy in predicting waste heat availability within the CC unit. Even though Model I underestimates the CO_2 flow rate by approximately 9 % and consequently overestimates the SRD, its accurate representation of waste heat availability and at the same time reasonable agreement with other key parameters make it the preferred choice.

As the main heat source considered for the heat pumps (chapter Section 3.1), correctly estimating the waste heat available at the overhead condenser is a critical aspect of this work. Again Model I provides results that are the most accurate to the experimental references. A detailed calculation of overhead stripper vapor composition, presented in section S3.1 in the SI, enables the accurate estimation of the H_2O:CO_2 mole fraction, essential for determining the high-quality waste heat available at the overhead condenser.

Ultimately, Model I (ENRTL-RK) was chosen for this study, with the intention of further refining and fine-tuning the model in future work.

4.2. Electrification scenarios

The electrification concepts are developed on the premise of a validated simulation. The pressure determines the boiling point of the rich amine solution, indirectly fixing the required temperature level to supply heat to the reboiler ($\Delta T = 11^{\circ}C$, see Section 3.2). To facilitate modeling and analysis, it was assumed that the superheated steam at 3 bar_a ($T_{sat} = 132.8^{\circ}C$, $\Delta T_{sup} = 23.2^{\circ}C$) is used as the sole hot utility in the system (Faramarzi et al., 2017), generated through the combustion of natural gas.

The process and performance parameters of base case as well as their electrified variants are summarized in Table 2. For higher degrees of electrification, the demand of both hot and cold utilities are lower, signifying a lower reliance on fossil-based energy sources. It is interesting to note that the single-stage variants (V1.1 and V2.1, see Fig. 5(a)), present different degrees of electrification at the same evaporator temperature (T_{EV1}), which can be attributed to a higher water content in the regenerator top gas for V2.0, providing a larger latent heat potential ($\dot{Q}_{source1}$).

The choice of working fluids fell on hydrocarbons (isopentane and n-butane) for the high-pressure operation, and ammonia for the low-pressure electrification scenarios. The choice of working fluid rested on the estimated heat pump COP and temperature lift (ΔT_{lift}), while simultaneously avoiding the use of deprecated refrigerants and proprietary substances. As seen in Table 2, the COP for V1 electrified variants decreases with a higher degree of electrification due to the increased temperature lift. Since available waste heat at higher temperatures (T_{EV1}) is limited, more thermal energy is required at lower temperatures (T_{EV2}), resulting in a higher flow rate of the working fluid, which ultimately leads to a higher requirement for compression power. An increased ΔT_{lift} leads to higher working fluid flow rates and power demands in the compressor, thus impacting the estimated COP of the heat pump. Due to the lower ΔT_{lift}, as well as better available heat quality at T_{EV1}, ammonia-based heat pumps (V2) present better COP values than hydrocarbon-based solutions.

The value of the pressure lift (ΔP, Table 2) is important to evaluate the practicality of the compressor design, and will influence the technology selection (for both compressors and heat exchangers) and thus the equipment costs.

Keeping in mind that the heat demand of V2.0 is around 29 % higher than V1.0 for the same amount of CO_2 removal, it is important to evaluate the availability of low-quality waste heat ($\dot{Q}_{source2}$). V1 variants are able to use 19 % of the total hot utility demand available as low-grade waste heat ($\dot{Q}_{source1}$) at high-temperature level (T_{EV1}), while V2 variants can use 30 % of the amount. Moreover, when evaluating the reduction in consumption of cooling water, complete electrification leads to a reduction of 35 % for V1.3 in comparison to V1.0, and 72 % for

Table 2
Characteristics of HTHP for each electrification concept. V1.0 and V2.0 correspond to systems where no degree of electrification is considered. Parameters of the reboiler: V1 — Pressure = 1.91 bar_a, Duty = 3417 kW, Temperature = 122° C; V2 — Pressure = 1.01 bar_a, Duty = 4417 kW, Temperature = 102° C. Steam condensation temperature: V1 — 133° C, V2 - 133° C.

Parameter	Unit	V1.0	V1.1	V1.2	V1.3	V2.0	V2.1	V2.2	V2.3
Degree of Electrification	%	0	27	50	100	0	38	50	100
Cold Utility	kW	5136	4486	4190	3356	6129	4779	4413	1704
Hot Utility	kW	3417	2497	1707	0	4417	2728	2207	0
SRD	$MJ/kgCO_2$	4.08	4.08	4.08	4.08	5.27	5.27	5.27	5.27
# HTHP stages		–	1	2	2	–	1	2	2
Working Fluid		*Steam*	Isopentane	*n*-Butane	*n*-Butane	*Steam*	Ammonia	Ammonia	Ammonia
COP		–	3.4	2.24	1.84	–	4.97	4.48	3.29
$\dot{Q}_{sink}$	kW	–	920	1710	3417	–	1689	2210	4417
P_{CD}	bar_a	2.97	13.87	27.72	27.72	2.97	80.14	80.14	80.14
T_{CD}[a]	°C	133	133	133	133	133	113	113	113
P_{EV1}	bar_a	–	3.56	8.09	8.09	–	33.12	33.12	33.12
T_{EV1}	°C	–	70	70	70	–	70	70	70
$\dot{Q}_{source1}$	kW	–	650	650	650	–	1350	1350	1350
$W_{comp,1}$	kW	–	270	599	1197	–	339	444	887
P_{EV2}	bar_a	–	–	3.78	3.28	–	–	20.33	13.50
T_{EV2}	°C	–	–	40	35	–	–	50	35
$\dot{Q}_{source2}$	kW	–	–	296	910	–	–	366	1725
$W_{comp,2}$	kW	–	–	165	660	–	–	50	454
$\Delta P_{1\text{-stage}} = \frac{P_{CD}}{P_{EV1}}$		–	3.89	–	–	–	2.42	–	–
$\Delta P_{2\text{-stage}} = \frac{P_{CD}}{P_{EV2}}$		–	–	7.32	8.44	–	–	3.94	5.94
$\Delta T_{lift,1\text{-stage}} = T_{CD} - T_{EV1}$		–	63	–	–	–	43	–	–
$\Delta T_{lift,2\text{-stage}} = T_{CD} - T_{EV2}$		–	–	93	98	–	–	63	78

[a] T_{CD} specifically refers to the condensation temperature of the working fluid, and should not be confused with the superheat temperature at the inlet of the condenser

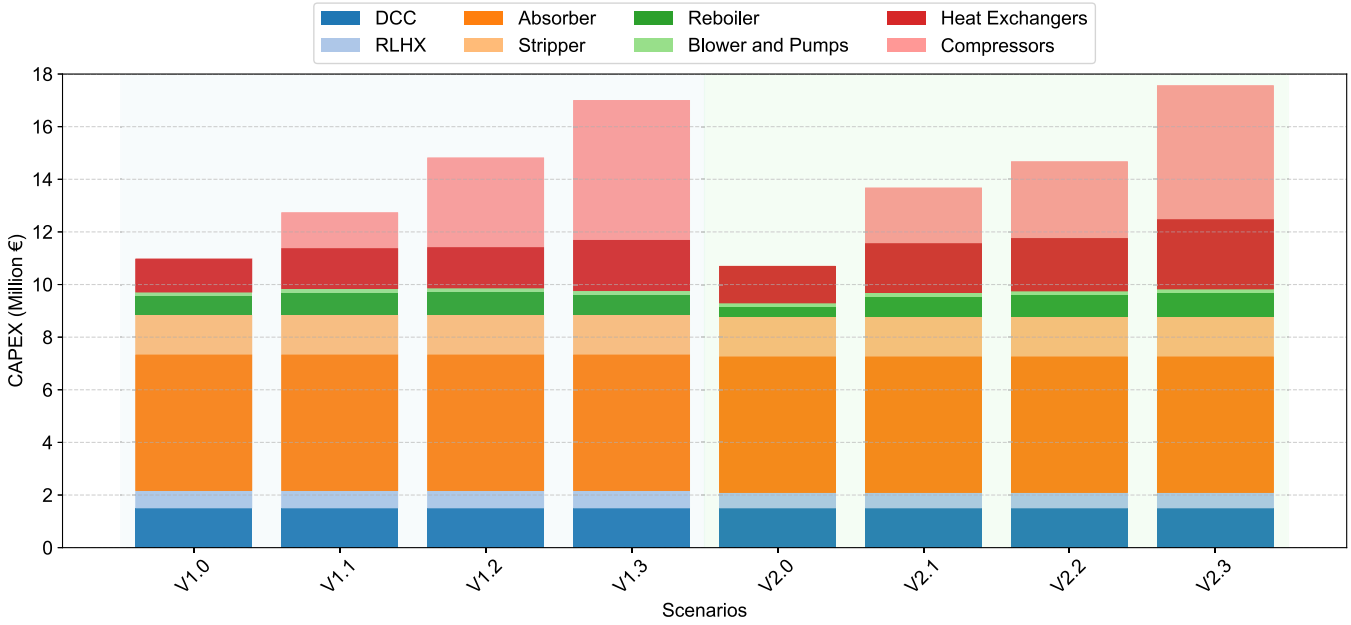

Fig. 6. Total CAPEX of the different scenarios with relative installed cost of equipment.

V2.3 in comparison to V2.0; the savings potential may be significant for industries located in areas with limited access to cooling water.

4.3. Economic analysis

4.3.1. CAPEX analysis

The total capital expenditure of the different scenarios is shown in Fig. 6. The bulk of the investment is associated with the core process equipment that is common to all cases, namely the absorber, stripper, direct-contact cooler (DCC) and the re-heat low-temperature heat-exchanger (RLHX). These items follow the same cost trend reported by Barlow et al. (2025) and exhibit only minor variations across the alternative scenarios.

Heat-pump installations frequently contain ancillary items that are not directly part of the working-fluid loop, such as compressor-cooling systems, buffer tanks, desuperheaters and sub-coolers (Flynn et al., 2011). As Winskel et al. (2024) point out, reliable cost data for commercial heat-pumps are scarce, which makes it difficult to produce trustworthy estimates for novel concepts like those examined in this manuscript. Nevertheless, a number of heuristic cost-correlations are available, usually expressed as a function of the delivered heat duty. Arpagaus et al. (2022) review several of these correlations and propose their own formulation.

Hydrocarbon-based heat pumps and refrigeration systems are technologically mature and are commercially available as plug-in solutions covering a wide spectrum of heat-load capacities and temperature levels. Their widespread adoption, however, is hampered by the inherent flammability and explosiveness of the hydrocarbon working fluids, which necessitate compliance with ATEX/IECE$_X$ standards and consequently raise equipment costs (Centre, 2023).

Ammonia-based reverse-Rankine HTHPs encounter a different set of obstacles when applied to high-temperature heat delivery. As highlighted by Ahrens et al. (2019), ammonia exhibits significant corrosivity and flammability at elevated temperatures, and commercial-grade ammonia often contains trace amounts of water that can impair compressor performance under high-discharge-temperature conditions. Moreover, the scarcity of cost-effective compressors capable of handling ammonia at the high pressures required for temperature lifts above 100° C has confined the commercial use of ammonia-driven systems largely to low-grade heat upgrading (Flynn et al., 2011; Centre, 2023).

In the present study the capital cost of a heat-pump is therefore taken as the sum of the costs of its main-loop constituents evaporator, compressor and condenser. Costs associated with expansion valves, safety-system hardware and other auxiliary equipment have been omitted from the analysis.

The biggest factor driving up the CAPEX of the electrified scenarios is the compressor. Compared to single-stage compressors, there is little literature available to estimate the costs of multi-stage compressors. In the context of this CAPEX analysis, the cost of the compressor unit is assumed to the sum of the installed costs of each stage, which were modelled separately. The two-stage compressors considered in this work present significant reductions in COP with increasing electrification, leading to cost increases of 150 % (V1.2) and 290 % (V1.3) versus V1.1, or 38 % (V2.2) and 141 % (V2.3) versus V2.1. For the complete electrification scenarios, the CAPEX of the compressors alone are comparable to the costs of the absorber column, traditionally the most expensive piece of equipment in this type of CC unit, corresponding to almost half of the CAPEX of the unit (Barlow et al., 2025; Ali et al., 2018).

All HX except RLHX and reboiler are grouped together and represented as “Heat Exchangers” in Fig. 6, where it can be observed that the costs increase visibly with higher degrees of electrification (increases of 20 % (V1.1), 21 % (V1.2), and 51 % (V1.3) versus V1.0; and 33 % (V2.1), 43 % (V2.2), and 88 % (V2.3) versus V2.0). This progressive increase in costs can be attributed to more number of HX’s (Fig. 5) with larger heat transfer areas, due to our definition of a low $\Delta T_{\min}$ (Fig. 3). The operating pressure (increased f_P, Table S17 in the SI) plays a bigger factor in the costs of V2 variants, due to the need for reinforced equipment. The reason can be verified by consulting the results shown in Table 2, where ammonia maintains a relatively high evaporation operating pressure even when the evaporator temperature is low.

At a first glance, it would be expected that a similar pattern would be seen for the reboiler(s). When analysing the non-electrified variants, it can be observed that the V2.0 reboiler is about 50 % more economic than the one employed by V1.0 (Fig. 6), due to a smaller heat transfer area permitted by a higher ΔT between the heat source (steam) and the boiling fluid (see Table 2).

Regarding the electrified variants, the values do not vary appreciably with the degree of electrification for the V1 scenarios (increases of 19 % (V1.1), 22 % (V1.2), and 8 % (V1.3) versus V1.0), but seem to do so for V2 scenarios (increases of 106 % (V2.1), 121 % (V2.2), and 141 % (V2.3) versus V2.0). The escalation observed for the V1 scenarios are mostly attributable to an increase in the number of equipment pieces (1 to 2), where one unit is covered by traditional utility and the other unit is covered by working fluid of heat pump. The increment in pressure is expected to play a smaller role in the equipment costs for V1 when compared to V2 (Table 2).

The nature of the phase change phenomenon at the condenser of the heat pump, supplying heat to the reboiler, may help explain the high costs of the ammonia-based reboilers (V2), as the choice of this working fluid significantly influences both the latent heat and sensible heat distribution. While heat supply in V1 scenarios occurs primarily through condensation of hydrocarbons, the high degree of superheating in the compressed NH_3 vapor (Fig. 4(b)) means that a large degree of sensitive heat contributes to the supply to the heat sink (reboiler) in V2 scenarios. While this factor leads to a higher LMTD, lowering the expected heat transfer area of the heat exchangers, the high pressure (f_P) and temperature factors (f_T) lead to more elevated heat exchanger costs for the V2 scenarios when compared to the V1 ones.

4.3.2. OPEX analysis

The results of the OPEX analysis for the different scenarios is presented in Fig. 7. The graphics show that the annual costs are dominated by the consumption of energetic utilities, either electricity or steam (68-77 % of total OPEX). The labor costs are significant but constant between the different scenarios. The feedstock costs are mostly dependent on cooling water make-up costs, but do not represent a significant fraction of the total annual OPEX. The yearly maintenance costs are defined as a fixed fraction of the total annualized CAPEX (4 %), leading to them constituting a relevant part of the annual OPEX.

When evaluating electrification variants of V1.0, an increasing trend in relative energy costs is visibly observed in Fig. 7, i.e., 10 % (V1.1), 26 % (V1.2), and 62 % (V1.3). The chief reason for the higher energy cost is the amplified electricity demand, which stems from the sharper reduction in COP at elevated electrification levels (Table 2). Contrarily, all V2 scenarios present a decreasing trend of utility costs with higher degrees of electrification (−4 %, −7 %, and −8 %, for V2.1, V2.2, V2.3, respectively, in comparison to the value found for V2.0). The high COP of the ammonia-based HTHP (Table 2) combined with greater electrification coverage reduces utility costs.

Walden and Padullés (2024) discuss the concept of price ratio (r_p, Eq. (12), where p_{el} refers to the price of electricity and p_{fuel} to the price of natural gas, see Table S18 in the SI) as a measure of the relative costs of electrification vs fossil fuel usage for the same amount of energy provided. As a rule of thumb, electrified configurations whose COP estimates are above r_p can be regarded as operationally cost-effective alternatives to fuel-based systems (Walden and Padullés, 2024).

$$r_p = \frac{p_{\text{el}}}{p_{\text{fuel}}} \tag{12}$$

The average r_p for Germany for the second half of 2024 was 4.72 for the cases not considering electrification (V1.0, V2.0), and 3.12 for all others, due to the comparatively higher power demand (Fig. 7). It must be kept in mind that these values refer to the use of the electricity from the grid, as the power demand can hypothetically be total or partially provided using photovoltaic or other renewable sources (Bernath et al., 2019).

4.3.3. Scenario/case comparison

Fig. 8 compares the trends of the capture cost and the process emissions for each scenario, considering both Scope I (direct emissions, including fuel use and non-captured CO_2 and Scope II (indirect emissions associated with the production and transport of electricity) emissions in Germany. Under each graph, the reader can find a table summarizing the key findings in the form of relative difference (Δ) to the base case (V1.0 or V2.0).

CO_2 emissions are generally higher for V2.0 than V1.0, due to a higher SRD (Table 2). V2 cases, using ammonia, present higher emissions due to a higher steam use at equivalent electrification levels, but fully electrified V2.3 presents lower emissions than V1.3 due to a lower electricity demand, associated with a higher COP (Table 2).

Fig. 8 also presents the evolution of the LCOC before (red, wide dash) and after (red, narrow dash) taking into account possible revenue from

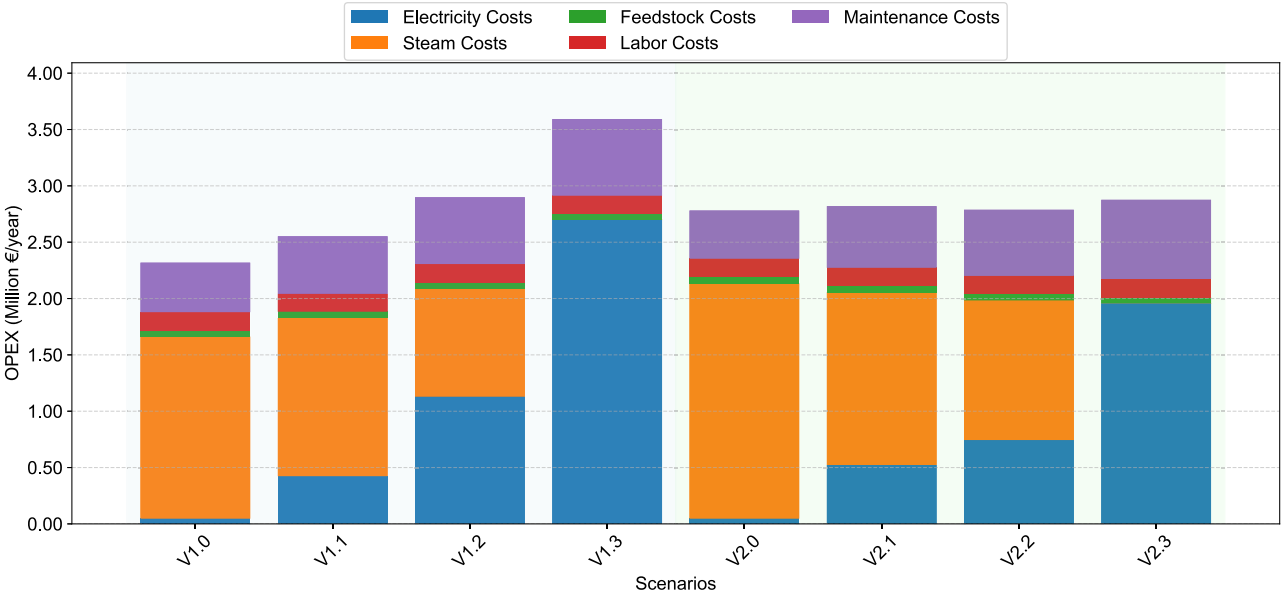

Fig. 7. Yearly OPEX of the different scenarios with relative cost components.

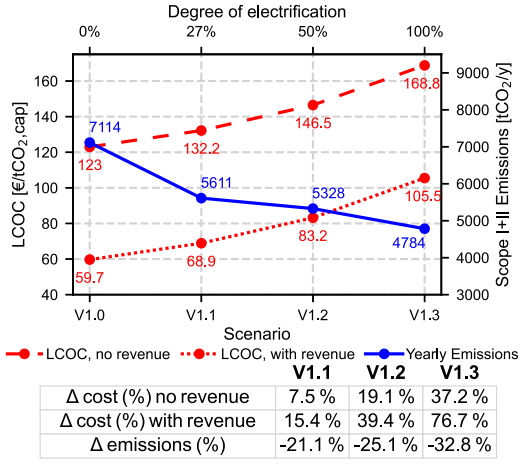

	V1.1	V1.2	V1.3
Δ cost (%) no revenue	7.5 %	19.1 %	37.2 %
Δ cost (%) with revenue	15.4 %	39.4 %	76.7 %
Δ emissions (%)	-21.1 %	-25.1 %	-32.8 %

(a) Scenario 1: Regenerator @ 1.91 bar_a

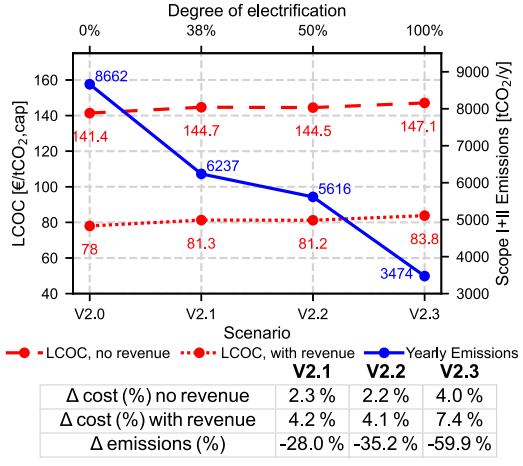

	V2.1	V2.2	V2.3
Δ cost (%) no revenue	2.3 %	2.2 %	4.0 %
Δ cost (%) with revenue	4.2 %	4.1 %	7.4 %
Δ emissions (%)	-28.0 %	-35.2 %	-59.9 %

(b) Scenario 2: Regenerator @ 1 atm_a

Fig. 8. Annual CO_2 capture cost and total CO_2 emissions for different degree of electrification of a standalone CC unit based in Germany.

the sale of excess EUA (Section 2.3.3). The two curves are plotted side-by-side to highlight the financial impact of carbon credits on highly polluting sectors such as conventional power generation.

A direct cross-scenario comparison (V1 vs. V2) is complicated by the distinct working fluids and energy-demand profiles adopted in each family. The LCOC for Scenario V1 (Fig. 8(a)) exhibits a comparatively pronounced upward trend that is tightly linked to the requirement for larger, more power-intensive compressors as the degree of electrification increases (Table 2). In comparison, Scenario V2 (Fig. 8(b)) shows only a very mild positive slope, indicated by the considerable difference seem in Δ_{cost} values.

At low electrification levels, the V1 Scenario presents the most favorable results for both emissions and costs, while the capture cost of the fully electrified scenario in V2 is comparable to that of the 50 % electrified scenario in V1, emitting a very similar amount of CO_2. Case V1.3 presents higher specific CC costs without delivering commensurate emission benefits. These findings further underscore the economic feasibility of operating the regenerator column at low pressure. This suggests that the fundamental concept of partial electrification can be achieved cost-effectively using waste heat within the CC system. Since the LCOC analysis is based on fixed energy costs that are determined by the location of the CC facility (in our case, Germany), the HTHP integration results can be equivocal. The same argument applies to yearly emissions, as the energy footprint can also vary. Therefore, the importance of sensitivity analysis comes into play which is covered in the next section.

4.3.4. *Sensitivity analysis*

Due to the absence of a traditional revenue stream, we conducted one-way deterministic sensitivity analyses considering the impact of several factors in both process cost and emissions. This technique isolates the influence of individual factors on the variation of the final metric, and no factor interaction was considered (Vreman et al., 2021).

Cost analysis — The first sensitivity analysis quantifies how the levelized cost of carbon capture (€/$t_{CO_{2,cap}}$) deviates from the baseline values shown in Fig. 8, with the results being summarised in Fig. 9, where Fig. 9(a) and (b) refer to the cost before accounting for revenue from the sale of EUA allowances. In each *spider-plot*, the spokes correspond

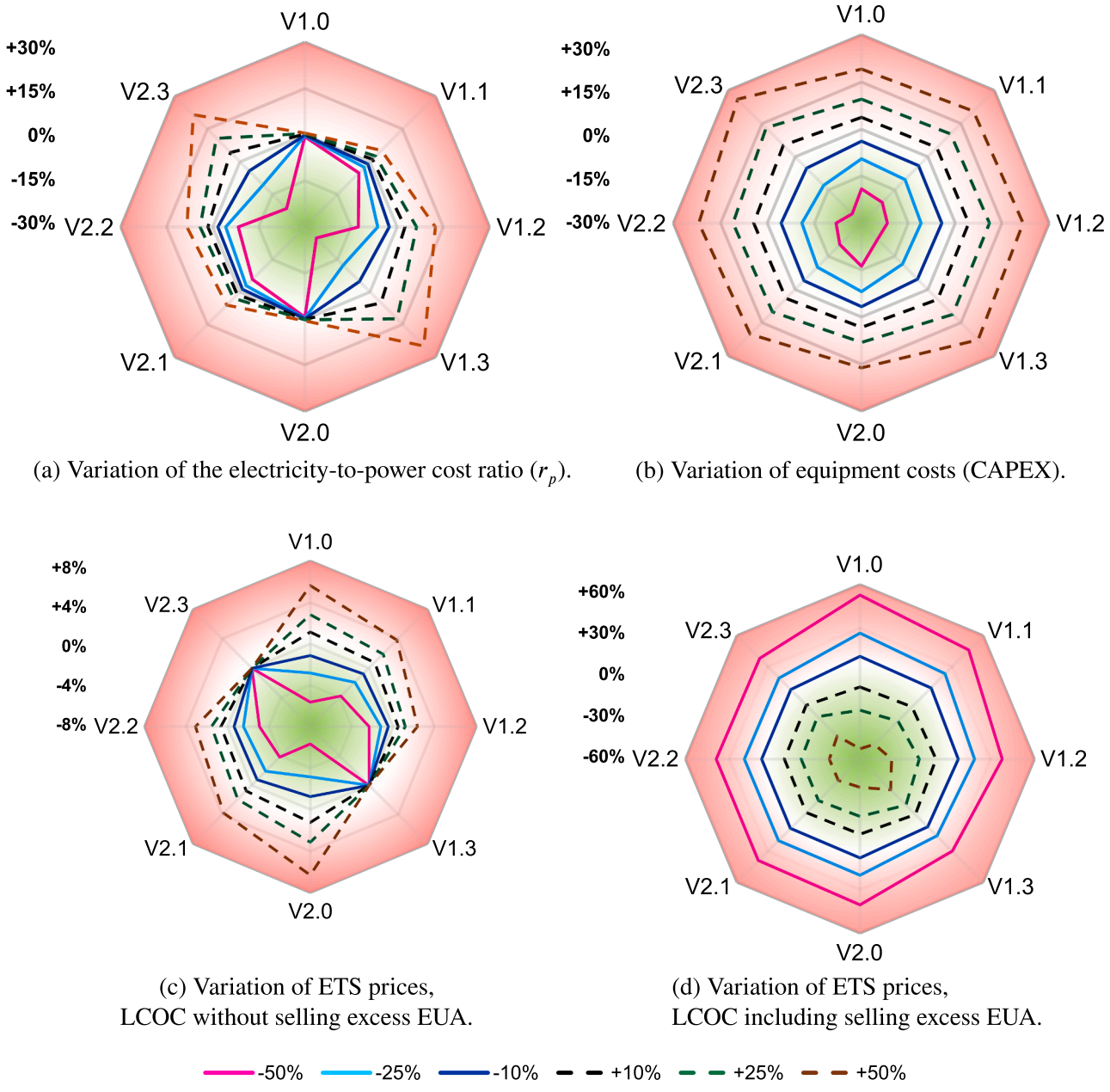

(a) Variation of the electricity-to-power cost ratio (r_p).

(b) Variation of equipment costs (CAPEX).

(c) Variation of ETS prices, LCOC without selling excess EUA.

(d) Variation of ETS prices, LCOC including selling excess EUA.

Fig. 9. One-off sensitivity analysis of the levelized cost of carbon capture (€/$t_{CO_{2,cap}}$).

to the eight operating cases (V1.0–V1.3 and V2.0–V2.3), the radial distance indicates the relative change in LCOC, and the coloured gradient (green → white → red) visualise the magnitude and direction of the effect (redder = cost increase, greener = cost decrease). The lines correspond to the different variation scenarios (changes of ±50 %, ±25 %, ±10 % in regards to the original value). The r_p ratio was varied by keeping the fuel-price parameter fixed (Table S18 in the SI), and adjusting the electricity price accordingly. Fig. 9(a) shows that LCOC after heat-pump integration is highly sensitive to electricity price fluctuations, especially for the fully electrified configurations (V1.3 and V2.3). The V1 series (hydrocarbon-based) exhibits a larger response because of its lower COP at comparable electrification levels, which translates into a higher electrical demand and thus greater cost variability.

These findings underline the importance of national electricity-generation mixes and related policy frameworks. Using Germany as a case study, the grid cost is strongly influenced by the country's reliance on imported fossil fuels and the associated surcharge mechanisms. Consequently, policies that promote domestic renewable generation (solar, wind) and reduce import dependence can markedly lower the electricity component of LCOC (Bundesnetzagentur, 2025; Schindler et al., 2022). Recent work on a German medium-sized city demonstrates that retrofitting district-heating networks with biomass gasification reduces fossil-fuel imports and valorises local waste streams, further mitigating electricity-price exposure (Böhning, 2025).

Uniform perturbations on the equipment costs (Fig. 9(b), reference values in Fig. 6) produce an expected monotonic response: higher CAPEX leads to higher LCOC, while lower CAPEX reduces it, with higher base CAPEX being proportionally more affected (V1.3, V2.3). Because OPEX includes a maintenance component that scales with equipment cost (Section 4.3.2, Fig. 7), CAPEX variations also affect the operating-cost side, amplifying their overall influence on LCOC.

To mimic the volatility of the EU Emissions Trading System (ETS), the price of EUA allowances was varied before (Fig. 9(c)) and after

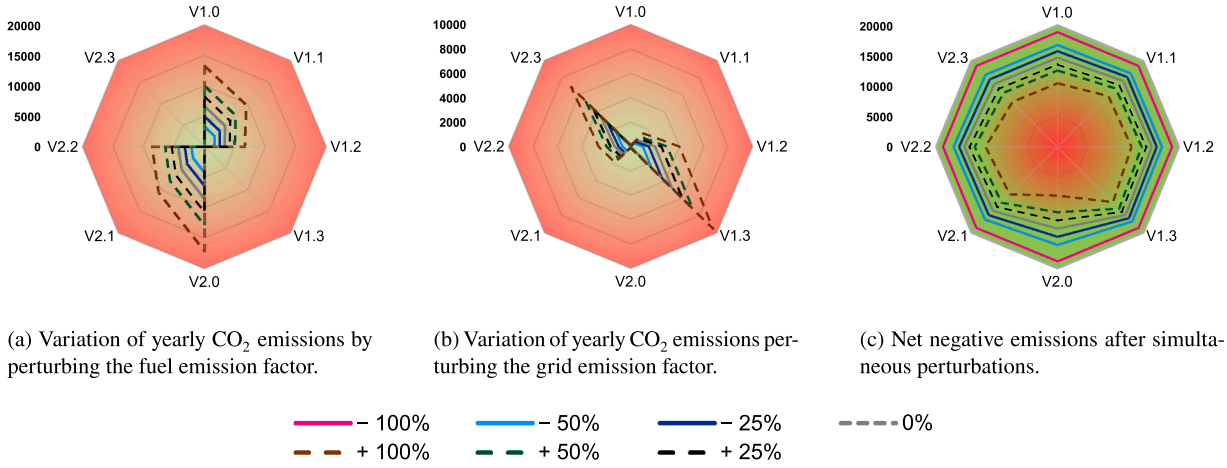

(a) Variation of yearly CO_2 emissions by perturbing the fuel emission factor.

(b) Variation of yearly CO_2 emissions perturbing the grid emission factor.

(c) Net negative emissions after simultaneous perturbations.

Fig. 10. One-off sensitivity analysis of scope I and II emissions. Results presented in Tonne $CO_{2,cap}$/y.

(Fig. 9(d)) accounting for the revenue generated by selling surplus allowances generated through carbon capture. Before accounting for this revenue (Fig. 9(c)), LCOC is more sensitive in low-electification cases, because these configurations present higher Scope I emissions (Section 4.3.3, Fig. 8). The trend reverses when accounting for this revenue (Fig. 9(d)), showing that higher EUA prices lead to lower net LCOC, as the additional revenue from sold credits outweighs the incremental process-emission costs.

Emissions analysis — The second set of sensitivity analyses quantifies how the two dominant emission sources, fuel combustion for the reboiler heat demand, and electricity-grid-associated emissions (Scope II, Fig. 10(b)), respond to perturbations in their respective emissions factors. As in Fig. 9, each *spider-plot*, displays eight operating cases (V1.0–V1.3 and V2.0–V2.3) along the spokes; however, the radial coordinate now represents the absolute emissions (Tonne$_{CO_{2,cap}/y}$), and the colour gradient fades to red with increasing emissions. The lines correspond to the different variation scenarios (±100 %, ±50 %, ±25 %, ±0 % relative to the baseline value).

By construction, fuel-related emissions (Fig. 10(a)) are zero for the fully electrified configurations (V1.3 and V2.3). A similar situation appears for the unelectrified configurations (V1.0 and V2.0) with respect to grid-associated emissions (Fig. 10(b)), but the values never reach zero because the flue-gas blower and process pumps still require electricity; the compressor demand absolutely dominates the grid-related share.

Perturbations of the specific fuel emission factor (Fig. 10(a)) emulate a change in fuel type: positive variations correspond to less efficient, more polluting fuels (e.g., coal, fuel oil), whereas negative variations represent cleaner alternatives (e.g., biomass, assumed carbon-neutral). At lower electrification rates, as was seen in Section 4.3.3, V2 cases exhibit a higher fuel demand and therefore a greater sensitivity to these fluctuations. These trends underline that, when a residual combustion stage is retained (i.e., low electrification), the fuel price translates linearly into the Scope I emissions; consequently, policy instruments that tax or subsidise the fuel can be used to modulate the net CO_2 balance of the plant.

Perturbations of the grid-emission factor (Fig. 10(b)) reflect changes in the national or local electricity mix. Positive variations indicate a higher share of carbon-intensive generation, while negative variations denote a larger share of renewables. Scope II emissions display an inverse behaviour to Scope I: they increase with the degree of electrification, as expected, and peak for the V1 cases due to lower COP (Section 4.3.3). Nevertheless, even the maximum Scope II emissions remain lower than those obtained from a +50 % increase in the fuel emission factor for the V2.0 and V2.1 cases.

A third graph (Fig. 10(c)) shows the net negative emissions after accounting for simultaneous perturbations of both emission factors with the same magnitude. In this representation, larger values correspond to greater net CO_2 removal, that is, a positive trend. The magnitude of the net-negative emissions is only weakly affected by the cost-parameter perturbations, reflecting the fact that the capture plant's capacity is fixed and that capture efficiency is only indirectly linked to economic drivers. Across all cases, ±100 % perturbations of the emission factors lead to total-emission variations of ±19-40 %. The most pronounced effect is observed for case V2.0 (±40 %), followed by V1.0 and V2.3 (±29 %). Importantly, the direction of the effect is uniform: any increase in the emission drivers reduces the net amount of CO_2 that can be captured, whereas cost reductions expand the capture envelope.

These observations highlight that, while the capture technology itself is technically robust, its economic viability, and consequently its contribution to net-negative emissions, depends critically on a favourable cost environment.

5. Discussion

5.1. New process configurations

The results presented in this manuscript are elaborated from the concepts described in a published patent (Rawat and Glade, 2025), which focused on the electrification of amine-based CC systems using reverse-Rankine HTHP solutions. Jensen et al. (2024) reported a COP value of 2.3 using isopentane for a heat pump system very comparable to the V1.3 scenario considered in this work (Table 2), employing similar technologies and working fluid, and exposing the potential conservatism displayed in the assumptions of this work. One crucial difference noticed during our evaluation was that the amount of waste heat available at the required temperature level in the overhead condenser was not sufficient to employ isopentane as a promising working fluid (due to issues of the working fluid entering the two-phase region during compression). However, if a certain amount of excess heat (greater than that estimated in this study) were available at this temperature level, isopentane would exhibit a much better COP than n-Butane, as reported in Table 2. However, the present work discusses a more complete methodology for identifying potentially high-quality heat sources (Section 3.1) and heat source broadening to maximize integration potential (Section 3.2). The methodology presented in this manuscript evaluates both single-stage HTHP integration and mixed heat sources (for two-stage HTHP), providing a roadmap for economical decarbonisation of the CC unit.

Alabdulkarem et al. (2015) stressed the significance of traditional pinch analysis and process integration when integrating HTHP systems into CC units, while outlining a method for selecting suitable working fluids for HTHP integration. In comparison, our methodology is comparatively more structured, underscoring the role of modest changes of process operational parameters (reboiler pressure) in tandem with the correct decision of working fluid to produce more economic or more extensive decarbonization scenarios (Section 3.3).

While the study focuses on reverse-Rankine cycle-based HTHP integration in CC unit, it deliberately does not compare its performance with MVR systems. Cremona et al. (2025) suggested that a combination of technologies featuring LVC, HTHP and MVR could be the most economically viable option, reinforcing the usefulness of leveraging waste heat from upstream and downstream units for the electrification of CC units. In contrast, the research presented in this manuscript prioritizes practical applicability and flexibility, by basing its analysis on a industrial-pilot scale, state-of-the-art test unit, and considering technologically mature HTHP solutions. In that sense, the study considers the evaluation of a standalone CC system, and evaluates available heat sources, providing valuable insights for equipment manufacturers aiming to electrify their CC units as well as for HTHP manufacturers seeking new market for application.

The potential of flexible adjustment of the regenerator pressure has been shown to allow for increasing oportunities for decarbonization of the amine-based CC unit. Despite operating at a non-optimum pressure, the V2.3 case leads to an overall more economically and environmentally balanced solution than integrating based on the base project. Although Jensen et al. (2024) suggested that below-atmospheric pressure operation could favor economic electrification, its higher energy demands may limit its practicality, but the results of this project may favor its applicability after considering standalone and process-chain-wide heat integration. The results presented in this work favor this perspective, as an initially unadvisable, albeit minor, modification of the regenerator pressure leads to a higher decarbonization potential for the integrated system at high electrification levels, while not being competitive at lower levels.

The capture costs reported in this study are higher than those from recent techno-economic analyses (TEA) reported by Cremona et al. (2025), Barlow et al. (2025), and Jensen et al. (2024). This discrepancy stems from an attempt to preserve the realism of the TCM pilot plant, which employs customisable columns, not a set of optimized, flue-gas-specific absorbers; this decision indubitably led to higher baseline energy consumption, providing a conservative safety margin for equipment operation. The campaign results considered as base for the modelling also only consider a capture rate of around 24 $kTonne_{CO2}$/y, corresponding to a yearly flue gas production of around 450 km^3/y. The values considered in the analysis are considered on the higher-end of the spectrum, to provide a safety margin for equipment operation.

Taking into consideration the practical aspects of HTHP installation, including replacing expansion valves with turbines, considering more complex levels of heat integration within HTHP system, among others can definitely improve the energetic efficiency as compared to results reported in this study. It is assumed that electricity is sourced from the power grid, enabling geographical flexibility in possible installation sites, and simulateously factoring in a potentially high grid-CO_2 footprint. This step intentionally limits the cost-effectiveness of the integrated CC proposal since, cheap electricity from renewables is not considered. Notably, the cost of the boiler is excluded from the CAPEX, whereas the installed cost of the HTHP is included, which may give the natural gas boiler option a cost advantage. The installed costs of compressors are expected to be unrealistically high, due to the limited availability of commercial HTHP units with intermediate gas intakes, like the ones we are considering (Tello-Oquendo et al., 2018). These two considerations are deliberate design choices, intended to frame the proposed scenarios from the viewpoint of technology suppliers, rather than a comprehensive system-level evaluation.

5.2. Policy and design implications

One-way deterministic sensitivity analyses was conducted considering the impact of important factors in both projected annual costs and expected process emissions, limited to the carbon capture process, independent of the industrial unit where it would be installed, and of any type of CO_2 conditioning taking place downstream.

Emissions and sensitivity analyses confirm that the carbon intensity of the electricity mix is the primary lever for the total CO_2 footprint of highly electrified capture systems, and that any policy-driven shift toward low-carbon electricity (e.g., renewable-energy mandates, carbon taxes on grid electricity) will have a proportionally larger impact on the V1-type configurations. In a situation like the one presented in this manuscript, the effect of electrical-grid-associated emissions must not be disregarded. Due to the nature of the electrical grid network in Germany, it is expected that cheaper electricity prices occur during times when renewable power can be produced at a lower cost (Energiewende, 2014), enabling the syncretism with the proposal by Isogai and Nakagaki (2024) to further minimize grid associated emissions. If that was achieved, a total CO_2 emissions could lower by a further 25 % for max electrification ammonia-based setups (V2.3). The most cost-effective path to deep decarbonisation is a combined approach that couples flexible stripper-pressure operation with low-carbon electricity procurement and prudent fuel-price management.

If the choice falls on the use of CC units at a low degree of electrification, the energetic penalty of using process steam to supply the heat demand of the CC unit must not be disregarded (Higgins and Liu, 2015). Modifying heat supply to make use of renewable source, such as biomass, synthetic bio-fuels, would lower Scope I emissions centered on the CC process, further improving the net-negative carbon balance. Rehfeldt et al. (2020) warns that fuel-switching comes with equipment costs and supply insecurities, due to the relative immaturity of the biomass market.

Other perspectives may fall on modifying the process equipment in a way that enables flexibility or reduces CAPEX while enabling modularity. Our results show that the emissions balance stays negative at very unfavorable conditions when viewed from the point of the standalone CC unit. Novel process configurations that enable flexibility on intermediate heat source tapping may enable the time-variation of the electrification level of the system, by varying the heat pump functioning.

It is important to keep the limitations of the study in mind. Not only are techno-economic assessments of the type often making very broad assumptions of the costs and dimensions of ancillary equipment in the real unit, this study is based on steady-state simulations developed to mimic a pilot plant. The analysis also assumes ideal behaviour in heat transfer and heat pump equipment, i.e., the U-factors and COPs would most likely be lower during operation. To finish, a cost analysis focused on the study of the carbon capture unit as a standalone unit does not include costs associated with the installation of such a unit to retrofit an existent industrial plant.

6. Conclusion

This study introduced a novel methodology for the cost-effective decarbonization of an amine-based carbon capture unit. The work entailed modeling of the 2015 campaign results reported by the TCM Mongstad research center, which employed an aqueous MEA solvent to treat a surrogate flue gas mixture representative of stack emissions from the natural gas-based CHP plant.

The methodology focuses, in opposition to several reports in the literature, on the ***standalone*** analysis of the CC unit to limit the need for external heat sources and maximize the installation and operation flexibility of our novel concept.

Without considering the effect of varying core operational conditions in the CC unit, state-of-the-art high temperature heat pumps (HTHP), employing n-Butane or isopentane as working fluids, can provide up to

27 % of the process heat demand, leading to a increase of around 7 % in the levelized cost of capture (LCOC), but a reduction of 21 % in process emissions.

The use of multi-stage heat pumps with intermediate heat sourcing, a solution of low technological maturity, would enable higher levels of decarbonization using more of available waste heat. When considering full electrification, the LCOC is expected to increase to 37 %, while leading to a reduction in the process emissions to 33 %, both values referring to the base CC unit.

It is well-known that minor adjustments in operational parameters within the CC process may lead to considerable differences in cost and energy demand, but may allow for considering wider heat pump integration scenarios. Although initially counterintuitive, our analysis showed that operating the regeneration column at P_{atm} instead of the base case (1.91 bar_a) increases the heat demand of the process. This, in turn, leads to higher emissions (22 %) and costs (15 %), however, it also enables the use of ammonia as a working fluid. A partial decarbonization of around 38 % was found using a single-stage HTHP solution, while the total decarbonization scenario using ammonia presented costs comparable to the 50 % electrification scenario using hydrocarbon-based heat pumps, while leading to an emissions decline of 60 % vs. the non-integrated ammonia case, or 51 % vs. the non-integrated process at normal pressure.

The effect of crediting unused carbon credits or emissions allowances in considerable lowering the estimated LCOC should not be disregarded. The installation of a CC unit based on the TCM Mongstad data would lead to a reserve of around 30,600 unspent EUA, corresponding to almost 2 million €/y (at ETS values from Dec 2024). If we assume that these credits are sold at market price, discounting the emissions associated with the operation of the CC unit, a positive balance of 1.5 M€/y would lead to an adjusted LCOC of 60 €/$t_{CO2,cap}$ for the base case, or 84 €/$t_{CO2,cap}$ after full electrification at adjusted pressure. Our sensitivity analysis indicates that costs would further drop by up to 40 %, if the ETS market prices would increase by 50 %. The opposite effect would be found for a stark decrease of the ETS prices, which could possibly be mitigated by government-backed carbon-credit price guarantees.

The fully electrified P_{atm} case also presented relevant savings in cooling water requirements, about 72 wt.% in comparison to the base case. This may allow future CC units to operate in areas where the supply of water is constrained.

The study presented in this manuscript assumes that the electricity is provided by the electrical grid at average contract prices. However, the current price ratio (r_p) in Germany does not favor electrification, nor do the specific emissions associated with a high consumption of fossil fuels for generation. Nonetheless, the results presented in this work show that complete electrification can be achieved with minor economic penalties. Further gains could been achieved if local renewable electricity was made available, or by the provision of further tax incentives or subsidies. In any case, it is not expected that the CC unit would reach financial break-even even when using 100 % renewable electricity at current ETS price trends.

This study highlights the importance of working fluid selection and stripper pressure on the overall energetic and economic performance of the unit. The introduction of the pressure ratio as a criterion for working fluid selection underscores the significance of practical application. The findings of this work provide a foundation for proprietary suppliers of CC technology to explore the development of electrified variants for CO_2 capture units that utilize waste heat within the system. The optimization of electrification potential and stripper operating pressure on the backdrop of increased energy consumption is an interesting direction for the future research. In essence, this also means investigating the potential for flexible adjustment of the stripper pressure, allowing it to operate between atmospheric and industrially optimized pressure levels, in order to leverage low electricity prices and enable dynamic electrification of carbon capture units. These results have significant implications for the decarbonization of industrial processes and the transition to a low-carbon economy.

CRediT authorship contribution statement

Shashank Singh Rawat: Writing – original draft, Visualization, Validation, Software, Methodology, Investigation, Formal analysis, Data curation, Conceptualization; **Frederico Gomes Fonseca:** Writing – review & editing, Investigation, Data curation; **María Isabel Roldán Serrano:** Writing – review & editing, Supervision, Investigation, Data curation, Conceptualization.

Data availability

Supplementary Information: Detailed simulation procedures, additional data, and supporting figures are available in the online version of this article. The datasets generated during and/or analysed during the current study are available from the corresponding author on reasonable request.

Declaration of Generative AI and AI-Assisted Technologies in the Writing Process

In the preparation of this manuscript, the authors have utilized large language models hosted by the scientific platform Helmholtz AI curated by the *Forschungszentrum Jülich*, and available for Helmholtz members through the Blablador platform. The authors confirm that the use of AI in this work was limited to language refinement and suggestions for rephrasing sentences, and that the conceptualization, methodology, analysis, and interpretation of the findings were conducted solely by the human authors. The responsibility for the content, including any errors or inaccuracies, lies entirely with the authors.

Declaration of competing interest

The authors declare the following financial interests/personal relationships which may be considered as potential competing interests. Shashank Singh Rawat is one of the registered inventors for the patent *Anlage und Verfahren zur Abtrennung von in einem Fluidstrom befindlichem Kohlenstoffdioxid* (DE102023208672A1) pending to the Deutsches Zentrum für Luft- und Raumfahrt (German Aerospace Center). All other authors declare that they have no known competing financial interests or personal relationships that could appear to influence the work reported in this paper.

Acknowledgements

This research did not receive any specific grant from funding agencies in the public, commercial, or not-for-profit sectors.

Supplementary material

Supplementary material associated with this article can be found, in the online version, at 10.1016/j.ccst.2025.100517

References

Agency, I.E., 2023. Net Zero Roadmap: A Global Pathway to Keep the 1.5°C Goal in Reach. Report 2023 Update. Technical Report. International Energy Agency. Paris, France. CC BY 4.0 licence. https://www.iea.org/reports/net-zero-roadmap-a-global-pathway-to-keep-the-15-0c-goal-in-reach.

Ahrens, M.U., Hafner, A., Eikevik, T.M., 2019. Development of ammonia-water hybrid absorption-compression heat pumps. In: 25th IIR International Congress of Refrigeration. IIF-IIR, France. https://doi.org/10.18462/iir.icr.2019.1869

Alabdulkarem, A., Hwang, Y., Radermacher, R., 2015. Multi-functional heat pumps integration in power plants for CO2 capture and sequestration. Appl. Energy 147, 258–268. https://doi.org/10.1016/j.apenergy.2015.03.003

Ali, H., Eldrup, N.H., Normann, F., Andersson, V., Skagestad, R., Mathisen, A., Øi, L.E., 2018. Cost estimation of heat recovery networks for utilization of industrial excess heat for carbon dioxide absorption. Int. J. Greenh. Gas Contr. 74, 219–228. https://doi.org/10.1016/j.ijggc.2018.05.003

Aromada, S.A., Eldrup, N.H., Normann, F., Øi, L.E., 2020. Techno-economic assessment of different heat exchangers for CO2 capture. Energies 13 (23), 6315. https://doi.org/10.3390/en13236315

Arpagaus, C., Bless, F., Bertsch, S., 2022. Techno-economic analysis of steam generating heat pumps for integration into distillation processes. In: 15th IIR-Gustav Lorentzen Conference on Natural Refrigerants (GL2022). Trondheim, NO. https://doi.org/10.18462/iir.gl2022.0029

Asian Development Bank, 2022. Study on Carbon Capture and Storage in Natural Gas-Based Power Plants. Technical Assistance Completion Report TA-9680. Asian Development Bank. Manila, Philippines. ADB Project No. 45096-001. https://www.adb.org/sites/default/files/project-documents//45096-001-tacr-02.pdf.

Aspen Technology, I., 2014. Rate-Based Model of the CO2 Capture Process by MEA using Aspen Plus. Aspen Technology, Inc. Bedford, MA, USA. Aspen Plus Documentation, Copyright (c) 2008-2014.

Aspen Technology, I., 2022. CO2 Capture from Coal Power Plant Using MEA and Aspen Plus. Aspen Technology, Inc. Bedford, MA, USA. Aspen Plus Documentation, Version V14.0, Copyright (c) 2022. http://www.aspentech.com.

Barlow, H., Shahi, S.S.M., 2024. State of the Art: CCS Technologies 2024. Technical Report. Global CCS Institute. Melbourne, Australia. https://globalccsinstitute.com/.

Barlow, H., Shahi, S.S.M., Kearns, D.T., 2025. Advancements in CCS Technologies and Costs. Technical Report. Global CCS Institute. https://www.globalccsinstitute.com/wp-content/uploads/2025/01/Advancements-in-CCS-Technologies-and-Costs-Report-2025.pdf.

Bejan, A., 1982. Second-law analysis in heat transfer and thermal design. In: Advances in Heat Transfer. Elsevier. Vol. 15, pp. 1–58. https://doi.org/10.1016/S0065-2717(08)70172-2

Bell, I.H., Wronski, J., Quoilin, S., Lemort, V., 2014. Pure and pseudo-pure fluid thermophysical property evaluation and the open-source thermophysical property library CoolProp. Ind. Eng. Chem. Res. 53, 2498–2508. https://doi.org/10.1021/ie4033999

Bernath, C., Deac, G., Sensfuß, F., 2019. Influence of heat pumps on renewable electricity integration: Germany in a European context. Energy Strategy Rev. 26, 100389. https://doi.org/10.1016/j.esr.2019.100389

Böhning, D., 2025. Steigerung der effizienz und wirtschaftlichkeit von holzvergasungsanlagen durch einsatz gering aufbereiteter waldrestholzer im rosenheimer verfahren zur holzvergasung. In: 28. Fachtagung “Nutzung Nachwachsender Rohstoffe – Biomasse - Wärme - Strom”. Zittau.

Bravo, J., Drapanauskaite, D., Sarunac, N., Romero, C., Jesikiewicz, T., Baltrusaitis, J., 2021. Optimization of energy requirements for CO2 post-combustion capture process through advanced thermal integration. Fuel 283, 118940. https://doi.org/10.1016/j.fuel.2020.118940

Bumb, P., Patkar, P.A., Mather, R., Kumar, R., Hall, J., Morton, F., Anthony, J., 2017. Field demonstration of advanced CDMax solvent at the US-DOE’s national carbon capture centre and the CO2 technology centre Mongstad DA, Norway. Energy Procedia 114, 1087–1099. https://doi.org/10.1016/j.egypro.2017.03.1261

Bundesnetzagentur, 2025. Energy Market Topics: Industrial Electricity Price Trends. https://www.smard.de/page/en/topic-article/5892/216044/industrial-electricity-price-trends. Accessed 28 August 2025.

Centre, H.P., 2023. IEA HPT Annex 58 - High-Temperature Heat Pumps: Task 1 - Technologies. https://heatpumpingtechnologies.org/annex58/wp-content/uploads/sites/70/2023/09/annex-58-task-1-technologies-task-report.pdf.

European Commission, DG CLIMA, 2014. About the EU ETS. https://climate.ec.europa.eu/eu-action/eu-emissions-trading-system-eu-ets/about-eu-ets_en.

Cremona, R., De Lena, E., Conversano, A., Spinelli, M., Romano, M.C., Gatti, M., 2025. Techno-economic assessment of high temperature heat pumps integrated in MEA-based post-combustion CO2 capture for cement plant. Carbon Capture Sci. Technol. 16, 100446. https://doi.org/10.1016/j.ccst.2025.100446

Díez, E., Langston, P., Ovejero, G., Romero, M.D., 2009. Economic feasibility of heat pumps in distillation to reduce energy use. Appl. Therm. Eng. 29, 1216–1223. https://doi.org/10.1016/j.applthermaleng.2008.06.013

Energiewende, A., 2014. Negative Electricity Prices: Causes and Effects. https://www.agora-energiewende.de/fileadmin/Projekte/2013/Agora_Negative_Electricity_Prices_Web.pdf.

Eunomia Research Consulting Ltd, Centre for Air Conditioning and Refrigeration Research (London Southbank University), 2014. Impacts of Leakage from Refrigerants in Heat Pumps. Department of Energy and Climate Change (DECC), UK Government London, United Kingdom, Final Report prepared for the UK Department of Energy and Climate Change. https://assets.publishing.service.gov.uk/media/5a7e1935ed915d74e622417e/Eunomia_-_DECC_Refrigerants_in_Heat_Pumps_Final_Report.pdf.

Faramarzi, L., Thimsen, D., Hume, S., Maxon, A., Watson, G., Pedersen, S., Gjernes, E., Fostå s, B.F., Lombardo, G., Cents, T., Morken, A.K., Shah, M.I., de Cazenove, T., Hamborg, E.S., 2017. Results from MEA testing at the CO2 technology centre Mongstad: verification of baseline results in 2015. Energy Procedia 114, 1128–1145. https://doi.org/10.1016/j.egypro.2017.03.1271

Federal Ministry for Economic Affairs and Climate Action (BMWK), 2023. Carbon Market Enables Efficient Climate Protection. https://www.bundeswirtschaftsministerium.de/Redaktion/EN/Dossier/kohlenstoffmarkt-effiziente-umsetzung-klimaschutz.html.

Flynn, J., Gladis, S., Buynacek, B., 2011. White Paper: Industrial Heat Pumps: Strategies for Decarbonizing Space and Water Heating Using Heat Pump Technology. https://media.copeland.com/1da81099-2c21-4ce5-8096-b16d0037b111/VILTER%20Heat%20Pump%20White%20Paper.pdf.

Goh, D., Gordon, N., 2025. Introducing Carnegie’s Revamped Climate Protest Tracker. https://carnegieendowment.org/emissary/2025/05/climate-protest-tracker-data-trends.

Golmen, L.G., Hjermann, D.Ø., Ledang, A.B., 2013. Two Years of Continuous Metocean Measurements at Mongstad, Norway, 2011-2013. Summary Report. Summary Report. Norwegian Institute for Water Research. http://hdl.handle.net/11250/216451.

Hasan, M.M.F., Baliban, R.C., Elia, J.A., Floudas, C.A., 2012. Modeling, simulation, and optimization of postcombustion CO2 capture for variable feed concentration and flow rate. 2. Pressure swing adsorption and vacuum swing adsorption processes. Ind. Eng. Chem. Res. 51, 15665–15682. https://doi.org/10.1021/ie301572n

Higgins, S.J., Liu, Y.A., 2015. Co2 capture modeling, energy savings, and heat pump integration. Ind. Eng. Chem. Res. 54 (9), 2526–2553. https://doi.org/10.1021/ie504617w

Hume, S.A., Shah, M.I., Lombardo, G., Kleppe, E.R., 2021. Results from CESAR-1 testing with combined heat and power (CHP) flue gas at the CO2 technology centre Mongstad. In: TCCS-11 - Trondheim Conference on CO2 Capture, Transport and Storage. SINTEF Academic Press, Trondheim, NO, pp. 2387–4295. https://hdl.handle.net/11250/2786512.

Husebye, J., Brunsvold, A.L., Roussanaly, S., Zhang, X., 2012. Techno-economic evaluation of amine based CO2 capture: impact of CO2 concentration and steam supply. Energy Procedia 29, 381–390. https://doi.org/10.1016/j.egypro.2012.06.053

International Carbon Action Partnership, 2025. ICAP Allowance Price Explorer. https://icapcarbonaction.com/en/ets-prices. Accessed 27 August 2025.

IPCC, 2022. Summary for Policymakers. In: Shukla, P.R., Skea, J., Slade, R., Khourdajie, A.A., van Diemen, R., McCollum, D., Pathak, M., Some, S., Vyas, P., Fradera, R., Belkacemi, M., Hasija, A., Lisboa, G., Luz, S., Malley, J. (Eds.), Climate Change 2022: Mitigation of Climate Change. Contribution of Working Group III to the Sixth Assessment Report of the Intergovernmental Panel on Climate Change. Cambridge University Press, Cambridge, UK and New York, NY, USA. chapter 1, pp. 1–52. https://doi.org/10.1017/9781009157926.001

IPCC, 2023. Contribution of Working Groups I, II and III to the Sixth Assessment Report of the Intergovernmental Panel on Climate Change. Technical Report. IPCC. Geneva, CH. https://doi.org/10.59327/IPCC/AR6-9789291691647

Isogai, H., Nakagaki, T., 2024. Power-to-heat amine-based post-combustion CO2 capture system with solvent storage utilizing fluctuating electricity prices. Appl. Energy 368, 123519. https://doi.org/10.1016/j.apenergy.2024.123519

Itoh, J., Shiroko, K., Umeda, T., 1986. Extensive applications of the T-Q diagram to heat integrated system synthesis. Comput. Chem. Eng. 10, 59–66. https://doi.org/10.1016/0098-1354(86)85046-3

Jensen, E.H., Andreasen, A., Jørsboe, J.K., Andersen, M.P., Hostrup, M., Elmegaard, B., Riber, C., Fosbøl, P.L., 2024. Electrification of amine-based CO2 capture utilizing heat pumps. Carbon Capture Sci. Technol. 10, 100154. https://doi.org/10.1016/j.ccst.2023.100154

Johnsen, K., Kleppe, E.R., Faramarzi, L., Benquet, C., Gjernes, E., de Koeijer, G., de Cazenove, T., Morken, A.K., Fløe, N.E., Shah, M.I., Aronsson, M., Ullestad, Ø., 2019. CO2 product quality: assessment of the range and level of impurities in the CO2 product stream from MEA testing at technology centre Mongstad (TCM). SSRN Electron. J. https://doi.org/10.2139/ssrn.3365995

Kim, I., Hoff, K.A., Mejdell, T., 2014. Heat of absorption of CO2 with aqueous solutions of MEA: new experimental data. Energy Procedia 63, 1446–1455. https://doi.org/10.1016/j.egypro.2014.11.154

Kishimoto, A., Kansha, Y., Fushimi, C., Tsutsumi, A., 2012. Exergy recuperative CO2 gas separation in pre-combustion capture. Clean Technol. Environ. Policy 14 (3), 465–474. https://doi.org/10.1007/s10098-011-0428-3

Kohl, A.L., Nielsen, R.B., 1997. Gas Purification. Elsevier. https://doi.org/10.1016/B978-0-88415-220-0.X5000-9

Linnhoff, B., Hindmarsh, E., 1983. The pinch design method for heat exchanger networks. Chem. Eng. Sci. 38, 745–763. https://doi.org/10.1016/0009-2509(83/80185-7

Linnhoff, B., Townsend, D.W., Boland, D., Hewitt, G.F., Guy, A.R., Marsland, R.H., 1994. A User Guide On Process Integration For The Efficient Use Of Energy. The Institution of Chemical Engineers. Rev. 1. Edition.

Luyben, W.L., 2018. Series versus parallel reboilers in distillation columns. Chem. Eng. Res. Des. 133, 294–302. https://doi.org/10.1016/j.cherd.2018.03.025

Luyben, W.L., 2022. Control of distillation columns with dual steam and hot-oil reboilers. Chem. Eng. Process. Process Intensif. 179, 109068. https://doi.org/10.1016/j.cep.2022.109068

Martin, G.R., Sloley, A.W., 1995. Effectively design and simulate thermosyphon reboiler systems: part 2. Hydrocarbon Process. 74. https://www.osti.gov/biblio/80160.

Maxwell, C., 2025. Cost Indices. https://toweringskills.com/financial-analysis/cost-indices/.

Mongstad, T.C., 2020. DOE-NETL’s 2020 Integrated Project Review Meeting. https://netl.doe.gov/sites/default/files/netl-file/20CCUS_Axel.pdf.

Mongstad, T.C., 2024. TCM DA’s Transparency Act Report 2023: Sustainable Testing of Technology for Capturing CO2. Technical Report. Technology Centre Mongstad. Published June 2024. https://gassnova.no/app/uploads/sites/5/2024/06/Transparency-Act-Report-TCM-DA.pdf.

Montañés, R.M., Fløe, N.E., Nord, L.O., 2017. Dynamic process model validation and control of the amine plant at CO2 technology centre Mongstad. Energies 10 (10), 1527. https://doi.org/10.3390/en10101527

Morgan, J., Chinen, A.S., Omell, B., Bhattacharyya, D., Deshpande, A., contributors, 2012–2022. Mea Steady-State Model (.bkp), version x.x (commit 698c22f2). https://github.com/CCSI-Toolset/MEA_ssm. Distributed under the CCSI Toolset license agreement — redistributions must retain copyright and disclaimers. Carbon Capture Simulation Initiative. Retrieved August 15, 2025.

Morgan, J.C., Soares Chinen, A., Omell, B., Bhattacharyya, D., Tong, C., Miller, D.C., Buschle, B., Lucquiaud, M., 2018. Development of a rigorous modeling framework for solvent-based CO2 capture. Part 2: steady-state validation and uncertainty quantification with pilot plant data. Ind. Eng. Chem. Res. 57 (31), 10464–10481. https://doi.org/10.1021/acs.iecr.8b01472

Morken, A.K., Pedersen, S., Kleppe, E.R., Wisthaler, A., Vernstad, K., Ullestad, Ø., Fløe, N.E., Faramarzi, L., Hamborg, E.S., 2017. Degradation and emission results of amine plant operations from MEA testing at the CO2 technology centre Mongstad. Energy Procedia 114, 1245–1262. https://doi.org/10.1016/j.egypro.2017.03.1379

Mullen, D., Braakhuis, L., Knuutila, H.K., Gibbins, J., Lucquiaud, M., 2024. Monoethanolamine degradation rates in post-combustion CO2 capture plants with the capture of 100 % of the added CO2. Ind. Eng. Chem. Res. 63, 13677–13691. https://doi.org/10.1021/acs.iecr.4c01525

Nakagaki, T., Isogai, H., Sato, H., Arakawa, J., 2019. Updated e-NRTL model for high-concentration MEA aqueous solution by regressing thermodynamic experimental data at high temperatures. Int. J. Greenh. Gas Contr. 82, 117–126. https://doi.org/10.1016/j.ijggc.2018.12.022

O'Brien, K., Krishnamurthy, K., Byron, M., Lu, Y., Bostick, D., Patel, V., Brownstein, S., Gioja, L., Dietsch, J., Guth, D., Larson, G., Nichols, J., Becker, P.J., 2021. Large pilot testing of Linde-BASF advanced post-combustion carbon dioxide capture technology at a coal-fired power plant. SSRN Electron. J. https://doi.org/10.2139/ssrn.3815230

Oexmann, J., Kather, A., 2010. Minimising the regeneration heat duty of post-combustion CO2 capture by wet chemical absorption: the misguided focus on low heat of absorption solvents. Int. J. Greenh. Gas Contr. 4, 36–43. https://doi.org/10.1016/j.ijggc.2009.09.010

Park, M.I., 2025. Technology Centre Mongstad – TCM. https://www.mongstadindustrialpark.no/mongstad-today/technology-centre-mongstad-tcm/. Year not specified in source.

Patkar, A., Bumb, P., 2017. Carbon clean solutions limited CDRMax CO2 capture technology: carbon capture technology for flue gas applications. In: AIChE Annual Meeting 2017. Minneapolis, MN, USA, pp. 1–48. Presented on July 18, 2017. https://www.aiche.org/system/files/aiche-proceedings/439541/papers/486212/P486212.pdf.

Peters, M.S., Timmerhaus, K.D., West, R.E., 2003. Plant Design and Economics for Chemical Engineers. McGraw-Hill Professional.

Prats-Salvado, E., Monnerie, N., Sattler, C., 2022. Techno-economic assessment of the integration of direct air capture and the production of solar fuels. Energies 15 (14), 5017. https://doi.org/10.3390/en15145017

Rawat, S.S., Glade, A., 2025. Anlage und Verfahren Zur Abtrennung Von in Einem Fluidstrom Befindlichem Kohlenstoffdioxid. Patent No. DE102023208672A1, Deutsches Zentrum für Luft- und Raumfahrt (DLR). Filing date: 2023-09-07. https://worldwide.espacenet.com/patent/search?q=pn%3DDE102023208672A1.

Rehfeldt, M., Worrell, E., Eichhammer, W., Fleiter, T., 2020. A review of the emission reduction potential of fuel switch towards biomass and electricity in european basic materials industry until 2030. Renew. Sustainable Energy Rev. 120, 109672. https://doi.org/10.1016/j.rser.2019.109672

Rochelle, G.T., 2009. Amine scrubbing for CO2 capture. Science 325, 1652–1654. https://doi.org/10.1126/science.1176731

Sanku, M.G., Svensson, H., 2019. Modelling the precipitating non-aqueous CO2 capture system AMP-NMP, using the unsymmetric electrolyte NRTL. Int. J. Greenh. Gas Contr. 89, 20–32. https://doi.org/10.1016/j.ijggc.2019.07.006

Schindler, D., Sander, L., Jung, C., 2022. Importance of renewable resource variability for electricity mix transformation: a case study from Germany based on electricity market data. J. Clean. Prod. 379, 134728. https://doi.org/10.1016/j.jclepro.2022.134728

Sema, T., Naami, A., Liang, Z., Shi, H., Rayer, A.V., Sumon, K.Z., Wattanaphan, P., Henni, A., Idem, R., Saiwan, C., Tontiwachwuthikul, P., 2012. Part 5b: solvent chemistry: reaction kinetics of CO2 absorption into reactive amine solutions. Carbon Manage. 3, 201–220. https://doi.org/10.4155/cmt.12.13

Smahi, A., Authier, O., Kanniche, M., Grandjean, L., Bouallou, C., 2023. Thermodynamic analysis of CO2 absorption in aqueous MDEA-PZ solution using ELECNRTL and ENRTL-RK models. Chem. Eng. Trans. 103, 631–636. https://doi.org/10.3303/CET23103106

Smith, R., 2005. Chemical Process Design and Integration. John Wiley & Sons, Ltd.

Tello-Oquendo, F.M., Navarro-Peris, E., Gonzálvez-Maciá, J., 2018. Optimization of the intermediate pressure for two-stage cycles with vapor-injection for subcritical and transcritical cycles. In: Proceedings of the 13th IIR Gustav Lorentzen Conference on Natural Refrigerants. Valencia, Spain, pp. 1–8. 8 pp.; Published June 18, 2018. https://doi.org/10.18462/iir.gl.2018.1268

Townsend, D.W., Linnhoff, B., 1983. Heat and power networks in process design. Part II: design procedure for equipment selection and process matching. AlChE J. 29, 748–771. https://doi.org/10.1002/aic.690290509

U. S. Environmental Protection Agency, Combined Heat and Power Partnership, 2015. Catalog of CHP Technologies. EPA Report EPA-430-R-15-001. U.S. Environmental Protection Agency. https://www.epa.gov/sites/default/files/2015-07/documents/catalog_of_chp_technologies.pdf.

Vreman, R.A., Geenen, J.W., Knies, S., Mantel-Teeuwisse, A.K., Leufkens, H. G.M., Goettsch, W.G., 2021. The application and implications of novel deterministic sensitivity analysis methods. PharmacoEconomics 39 (1), 1–17. https://doi.org/10.1007/s40273-020-00979-3

Walden, J.V., Padullés, R., 2024. An analytical solution to optimal heat pump integration. Energy Convers. Manage. 320, 118983. https://doi.org/10.1016/j.enconman.2024.118983

Walden, J.V., Wellig, B., Stathopoulos, P., 2023. Heat pump integration in non-continuous industrial processes by dynamic pinch analysis targeting. Appl. Energy 352, 121933. https://doi.org/10.1016/j.apenergy.2023.121933

Wilk, V., Leibetseder, D., Zauner, C., Rath, A., Schwaiger, M., 2024. Improving energy efficiency of carbon capture processes with heat pumps. Int. Sustainable Energy Conf. Proc. 1. https://doi.org/10.52825/isec.v1i.1083

Winskel, M., Heptonstall, P., Gross, R., 2024. Reducing heat pump installed costs: reviewing historic trends and assessing future prospects. Appl. Energy 375, 124014. https://doi.org/10.1016/j.apenergy.2024.124014

Xu, Q., Wu, J., Guo, Z., Xue, X., Li, X., 2022. Analysis of optimal intermediate temperature and injection pressure for refrigerant injection heat pump systems with economiser. Appl. Therm. Eng. 210, 118361. https://doi.org/10.1016/j.applthermaleng.2022.118361

Zhang, K., Liu, Z., Huang, S., Li, Y., 2015. Process integration analysis and improved options for an MEA CO2 capture system based on the pinch analysis. Appl. Therm. Eng. 85, 214–224. https://doi.org/10.1016/j.applthermaleng.2015.03.073